Distributed control for a multi-evaporator air conditioning system

Jun Mei[a,b,*], Xiaohua Xia[b]

[a] *School of Mathematics and Statistics, South-Central University for Nationalities, Wuhan 430074, China*
[b] *Centre of New Energy Systems, Department of Electrical, Electronic and Computer Engineering, University of Pretoria, Pretoria 0002, South Africa*

Abstract

An autonomous hierarchical distributed control (AHDC) strategy is proposed for a building multi-evaporator air conditioning (ME A/C) system in this paper. The objectives are to minimize peak demand and energy costs, and to reduce communication resources, computational complexity and conservativeness while maintaining both thermal comfort and indoor air quality (IAQ) in acceptable ranges. The building consists of multiple connected rooms and zones. The proposed control strategy consists of two layers. The upper layer is an open loop optimizer, which only collects local measurement information and solves a distributed steady state resource allocation problem to autonomously and adaptively generate reference points, for low layer controllers. This is achieved by optimizing the demand and energy costs of a multi-zone building ME A/C system under a time-of-use (TOU) rate structure, while meeting the requirements of each zone's thermal comfort and IAQ within comfortable ranges. The lower layer also uses local information to track the trajectory references, which are calculated by the upper layer, via a distributed model predictive control (DMPC) algorithm. The control strategy is distributed at both layers because they use only local information from the working zone and its neighbors. Simulation results are provided to illustrate the advantages of the designed control schemes.

Keywords:
Multi-evaporator air conditioning system, two-layer distributed controls, model predictive control, time-of-use, energy/demand reducing.

Nomenclature	
A_1	heat transfer area in the dry-cooling region of the DX evaporator, m^2
A_2	heat transfer area in the wet-cooling region of the DX evaporator, m^2
A_{win}	represents the total window area, m^2
C_a	specific heat of air, kJ kg^{-1} $^\circ C^{-1}$
C_c	CO_2 concentration in the conditioning space, ppm
C_{load}	pollutant load, m^3/s
C_s	CO_2 concentration of air supply, ppm
d	cross-sectional area of zone, m^2
G	amount of CO_2 emission by a person, L/h
h_{fg}	latent heat of vaporization of water, kJ/kg
h_{r1}	enthalpy of refrigerant at evaporator inlet, kJ/kg
h_{r2}	enthalpy of refrigerant at evaporator outlet, kJ/kg
h_s	enthalpy leaving the DX evaporator, kJ/kg
k_P, k_I	proportional and integral coefficients
m_r	mass flow rate of refrigerant, kg/s
M_{load}	moisture load in the conditioned space, kg/s

*Corresponding author. Tel.: +27 12 420 4353; fax: +27 12 362 5000
Email address: junmei027@gmail.com (Jun Mei)

$Occp$	number of occupants
Q_{load}	sensible heat load in the conditioned space, kW
Q_{rad}	solar radiative heat flux density, W/m^2
R	thermal resistance, °C/kW
T_d	air temperature leaving the dry-cooling region on air side of the DX evaporator, °C
T_{mix}	mixing temperature between the outside air and return air, °C
T_s	air temperature leaving the DX evaporator, °C
T_w	temperature of the DX evaporator wall, °C
T_z	air temperature in the conditioned space, °C
T_0	temperature of the outdoor air, °C
V	volume of the conditioned space, m^3
v_a	indoor air velocity, m/s
V_{h1}	air side volume in the dry-cooling region on air side of the DX evaporator, m^3
V_{h2}	air side volume in the wet-cooling region on air side of the DX evaporator, m^3
v_f	air volumetric flow rate, m^3/s
W_{mix}	mixing moisture content of outside air and return air, kg/kg
W_s	moisture content of air leaving the DX evaporator, kg/kg
W_z	moisture content of air-conditioned space, kg/kg
W_0	moisture content of the outdoor air, kg/kg
Greek letters	
α_{dc}	heat transfer coefficient between air and the DX evaporator wall in the dry-cooling region, kW m^{-2} °C^{-1}
α_{wc}	heat transfer coefficient between air and the DX evaporator wall in the wet-cooling region, kW m^{-2} °C^{-1}
ε_{win}	transmissivity of glass of window
ρ	density of moist air, kg/m^3
Subscripts	
i	room number
Abbreviations	
AHDC	autonomous hierarchical distributed control
DMPC	distributed model predictive control
EEV	electronic expansion valve
HVAC	heating, ventilation and air conditioning
IAQ	indoor air quality
ME A/C	multi-evaporator air conditioning
MPC	Model predictive control
NLP	nonlinear programming
PMV	predicted mean vote
PSA	pressure swing absorption
TABS	thermally activated building systems
TOU	time-of-use

1. Introduction

It is well known that many environmental problems are linked to energy consumption. The energy consumed by the building sector accounts for 40% of the total energy consumption in the world [1]. Among all building energy consumers, air conditioning (A/C) systems are responsible for the largest share, which represents close to 50% of the total electricity use in the building sector.

In recent years, many researchers have focused on reducing energy consumption of building heating, ventilation and air conditioning (HVAC) systems [2, 3]. Meanwhile, indoor comfort is also important for buildings, since it directly affects the occupants' working efficiency. The effective control of HVAC systems has the potential of reducing energy consumption or cost and improving indoor thermal comfort and air quality (IAQ). In [4], the authors proposed a method of real-time determination of an optimal indoor-air condition for the HVAC system to consider indoor thermal comfort and IAQ for occupants simultaneously with efficient energy consumption. However, this method is only tested around the desired points; we do not know if this method can be used without the desired points.

Model predictive control (MPC) has been verified as one of the most successful advanced control strategies, which is capable of improving energy efficiency and thermal comfort in buildings [5]-[10]. An energy-optimized open loop optimization and the MPC schemes were proposed [11, 12] for a direct expansion (DX) A/C system to improve energy efficiency while maintaining indoor thermal comfort and IAQ within comfort levels. Other advantages of MPC for building HVAC systems include robustness, tunability and flexibility [13]. Despite MPC having superior performance to other control strategies, the size of the optimization problem increases rapidly when the dimension of the building A/C systems is large. Centralized MPC techniques were proposed [14]-[17] for multi-zone HVAC systems to improve energy efficiency and thermal comfort. In the centralized control structure case, all the subsystems are controlled by one MPC law. The model used for prediction includes the coupling elements. When a centralized MPC algorithm is used for controlling HVAC systems in a large number of rooms, its algorithm is impractical since the optimization problems may not be solved in a reasonable time and the control systems are not easy to maintain. To reduce computational time, one of the effective predictive control strategies is a decentralized MPC approach [18]. Large-scale control problems are decomposed into several independent control problems, which can take care of the local control parameters [19]. However, the results demonstrated that the control performance loss was 28.58%. A distributed control approach is capable of balancing these issues. The structure of the distributed control is similar to a decentralized law, but is essentially a different approach [20]. The distributed control decomposes the centralized control to a group of local agents communicating with its neighbors, which makes it possible to be used for large-scale dynamically coupled systems. A communication network that allows collaboration among local control laws, which allows the improvement of global system performance compared to a decentralized structure. Moreover, computational demand should be significantly reduced compared to the centralized structure [21].

Owing to the advantages of distributed model predictive control (DMPC), this strategy was proposed to reduce the computational demand and handle the coupling among subsystems [22]-[25]. A DMPC was proposed in [23] to improve the energy efficiency of the HVAC system while keeping zone temperature within the comfort range. In the study, the nonlinear optimal control problem is formulated and solved through sequential quadratic programming. Then the subproblem is decomposed further by adopting a subgradient approach. A local controller reaches the optimal solution by repeatedly negotiating with its neighbours in every sampling period, which inevitably increases the demand for calculation. In [22], the DMPC algorithm, only required the predicted output exchanged with its neighbours for every sampling period. However, this algorithm can only obtain Nash equilibrium, which may not be the optimal solution. In [24], the authors proposed a DMPC algorithm to control multi-source multi-zone temperatures. In order to attenuate the online computational burden, the DMPC algorithm was implemented based on Benders' decomposition. The results show that the computational and convergence times of this algorithm are superior to the centralized MPC. However, the energy efficiency of the DMPC method is not particularly good compared to the centralized MPC strategy. Furthermore, this type of distributed structure does not converge to the optimal solution, as in [25] which was an agent-based suboptimal controller; the drawback is transmitted to the decomposition algorithm.

In addition to improving energy efficiency while maintaining building multi-zones' thermal comfort within comfort range, DMPC strategies based on energy scheduling were proposed in [26]-[27]. In [26], the authors proposed a method that combined the closed-loop centralized and distributed structures together to design a hierarchical control scheme to balance the computational complexity and conservativeness. In the study, the upper layer controller collects temperature and predictive information of all rooms and zones, which implies that the centralized scheduling (CS) needs to communicate with all rooms. The upper layer

optimization problem is nonlinear, and solving it for a large building using centralized approaches is computationally cumbersome, leading to scalability issues. Furthermore, implementing centralized approaches requires transmission of zone-levels models and sensor information to the CS, leading to engineering difficulties and increasing information exchange. In the lower layer, the distributed controller only uses one room's information and its neighbor off-line reference signals. This may cause loss of control accuracy in receding horizon. Moreover, the trajectory references in the optimization objectives are given and fixed over a 24-hour period, as in [22, 23, 25]. Centralized and distributed MPC controllers following fixed trajectory references were also reported in other field [28]. In our previous work [12], the results demonstrated that the MPC strategy following preprogrammed time-varying reference points can save more in energy consumption and cost when compared with a fixed trajectory reference. More recently, in [27], the authors proposed adaptive learning and distributed control together to improve the energy efficiency and thermal comfort for multi-zone HVAC systems. The optimal references are preprogrammed and time-varying, while the presented zone thermal dynamics of a multizone building did not consider the interaction between rooms. Moreover, this distributed optimization algorithm is solved by using the subgradient method.

Advanced building structures are extremely complicated, with widely equipped multi-evaporator (ME) A/C systems. An ME A/C, which is DX based, consists of an outdoor compressor and condensing, and multiple indoor units including electronic expansion valves (EEVs) and evaporators [29]. Experimental results have illustrated that the control performance of the novel capacity control algorithm is further improved in comparison with its previous work. However, controlling indoor air temperature by using the novel capacity control algorithm could still be subject to significant fluctuations under certain operating conditions because of using a temperature dead-band, time-delay for compressor start-up. The interaction with other indoor units may be an important impact factor but was rarely considered. To improve the energy efficiency of a multi-zone building ME A/C system, thermal comfort and IAQ levels, a suitable optimization method is required for making each room's temperature, humidity and CO_2 concentration consistent with their desired references. To realize it, we consider a case that each DX unit can exchange information with its neighbors.

To overcome the above issues, in this paper we present an autonomous hierarchical distributed control (AHDC) method for a multi-zone building ME A/C system which not only considers how to maintain multiple zones' thermal comfort and IAQ within comfortable ranges but also considers reduction of communication resources, computational complexity and conservativeness reduction, and energy consumption and costs. Meanwhile, the peak-average-ratio (PAR) can also be considered in this paper. Moreover, the proposed comfort control considers thermal comfort and IAQ and the coupling effects of them. This control strategy consists of two layers. The upper layer is open loop scheduling that collects only a room's measurement information containing room cooling and pollutant loads, weather conditions, end-user services including demand and energy rates, thermal comfort and IAQ levels and operation profiles. Then the upper layer formulates and solves a steady-state optimization problem for minimizing the demand and energy costs of the multi-zone building ME A/C system under a time-of-use (TOU) rate structure of electricity over a 24-hour period using nonlinear programming (NLP) algorithm. We make an assumption that the multi-zones are similar in the occupancies, functions and purposes; in this situation, one can distributively design an optimal scheduler. This scheduling generates time-varying trajectory references and communicates with the whole connected network through neighbors. All rooms then transmit their references to the lower layer controllers. The lower layer designed as DMPC controllers also uses local information to formulate and solve local optimization problems to track the autonomously and adaptively time-varying trajectory reference signals calculated by the upper layer. For simplicity, we make an assumption that all state variables are measured, thus full state feedbacks are considered. Our future work will consider designing observers in case some variables are not measured. The upper layer distributed way is different from the upper layer controllers in [26, 28], which need to collect all rooms' measurement information. It is also different from the distributed controllers in [21]-[25], which collect information from a zone and its neighbors. The proposed control scheme can be realised with reduced, cheaper and short-range communication modules, and depending on the communication topology, a receiver only. While in the conventional control schemes [21]-[25], [26, 28], it may require full-swing communication modules, i.e., with both a transmitter and receiver, which require external service providers in long-range data communication modules. The lower layer designs a new

distributed controller for a zone such that this subsystem depends entirely on the zone by introducing a new input variable over a short-term horizon. This distributed control scheme is desirable in practice and can be easily implemented by our previous control algorithm [12]. The results show that the proposed control scheme is superior to the previous control strategy on energy efficiency.

Our principal contributions can be summarised as follows:

1) We first propose two-layer distributed control strategies that not only reduce more energy demand and costs in comparison with previous works but also maintain both thermal comfort and IAQ of multi-zone within comfortable ranges. These levels of performance are demonstrated in the case study.

2) The proposed steady state distributed control and closed-loop distributed control schemes have the potential of reducing the complexity of computation and the hardware of communication modules in comparison with the centralised, non-distributed control schemes and hierarchical distributed control schemes.

3) A novel approach for the lower layer closed-loop distributed control is designed to obtain a new feedback controller. This is achieved by introducing new input variables such that the closed-loop distributed control subsystems can be converted to a subsystem that depends entirely on one zone and our previous MPC algorithm developed for a single zone can be used.

4) This study considers the predicted mean vote (PMV) index as an indicator of both thermal comfort and IAQ.

This paper is organized as follows: In Section 2, the nonlinear dynamical models and energy models for the multi-zone building ME A/C system, the PMV index and the system constraints are presented. The proposed AHDC method for the multi-zone building ME A/C system is proposed in Section 3. Simulation results are provided in Section 4. Section 5 concludes this paper.

2. System model

2.1. An ME A/C system in buildings

The schematic of an ME A/C system is illustrated in Fig. 1. The ME A/C system includes dampers, DX evaporators, an air-cooled tube-plate-finned condenser, a variable speed compressor, EEVs, variable speed centrifugal supply fans with pressure swing absorption (PSA) boxes, and a damper for mixing return air from the ME A/C system with outside air. The variable speed supply fan adjusts its own speed based on the air flow rate/opening controlled by EEV to control cooled air to each room. Each indoor unit placed in the room has an EEV and an evaporator. The PSA box regulates the conditioned air flow rate and absorbs CO_2 contaminant concentration for improving the fresh air ratio. Each indoor unit is connected to the variable speed compressor and the outlet of the air-cooled condenser. The indoor air unit recirculates return air from building spaces and mixes it with outside air. The proportion of return air to outside air is controlled by damper positions in the ME A/C system. The mixed air is cooled by the cooling coils.

Because of the complex nature of air flow and the heat transfer process, ME A/C systems are usually modelled as time-varying nonlinear partial differential equations [30], which are not suitable for control and optimization. Therefore, the following assumptions are made to simplify the modelling.

1) The air in each room and outdoor environment is well mixed immediately so that the temperature, humidity and CO_2 concentration distributions are uniform.

2) The heat capacity of air is constant.

2.2. Dynamic model of the ME A/C system

According to the above configuration, we use an undirected connected graph structure to represent the rooms and their dynamic couplings as described below. We associate the i-th room with the i-th node of the system. The mathematical dynamic models for the multi-zone building ME A/C system via the relationship between air enthalpy, temperature and the moisture content leaving the evaporator i of unit i as $h_{s,i} = C_a T_{s,i} + h_{fg} W_{s,i}$ are described as follows. In this paper, we only consider the interaction between rooms by sensible heat gain.

$$C_a \rho V_i \frac{\mathrm{d}T_{z,i}}{\mathrm{d}t} = \sum_{j=1}^{m} \frac{T_{z,j} - T_{z,i}}{R_{ij}} + \frac{T_0 - T_{z,i}}{R_i} + C_a \rho v_{f,i}(T_{s,i} - T_{z,i}) + Q_{load,i}, \tag{1a}$$

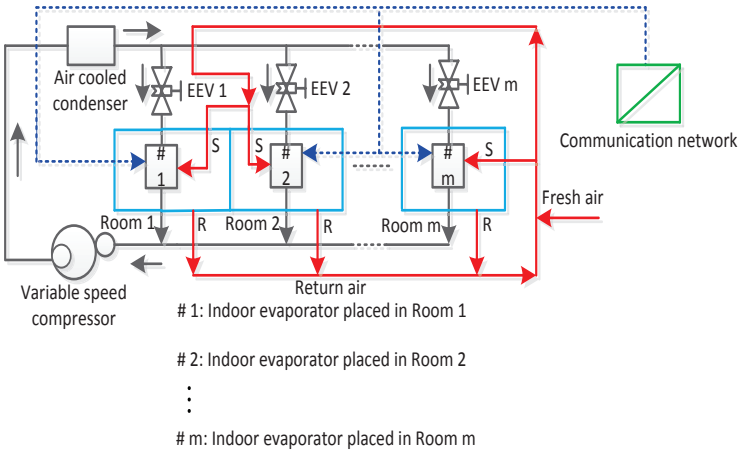

Figure 1: Schematic diagram of an ME A/C system.

$$\rho V_i \frac{\mathrm{d}W_{z,i}}{\mathrm{d}t} = \rho v_{f,i}\left(\frac{h_{s,i} - C_a T_{s,i}}{h_{fg}} - W_{z,i}\right) + M_{load,i}, \tag{1b}$$

$$C_a \rho V_{h1,i} \frac{\mathrm{d}T_{d,i}}{\mathrm{d}t} = C_a \rho v_{f,i}(T_{mix} - T_{d,i}) + \alpha_{dc,i} A_{1,i}\left(T_{w,i} - \frac{T_{mix} + T_{d,i}}{2}\right), \tag{1c}$$

$$\begin{aligned} \rho V_{h2,i} \frac{\mathrm{d}h_{s,i}}{\mathrm{d}t} =& \alpha_{wc,i} A_{2,i}\left(T_{w,i} - \frac{T_{d,i} + T_{s,i}}{2}\right) + h_{fg} \rho v_{f,i}\left(W_{mix} - \frac{h_{s,i} - C_a T_{s,i}}{h_{fg}}\right) \\ &+ C_a \rho v_{f,i}(T_{d,i} - T_{s,i}), \end{aligned} \tag{1d}$$

$$\begin{aligned} C_{w,i} \rho_{w,i} V_{w,i} \frac{\mathrm{d}T_{w,i}}{\mathrm{d}t} =& \alpha_{dc,i} A_{1,i}\left(\frac{T_{mix} + T_{d,i}}{2} - T_{w,i}\right) + \alpha_{wc,i} A_{2,i}\left(\frac{T_{d,i} + T_{s,i}}{2} - T_{w,i}\right) - \\ & (h_{r2,i} - h_{r1,i}) m_{r,i}, \end{aligned} \tag{1e}$$

$$V_i \frac{\mathrm{d}C_{c,i}}{\mathrm{d}t} = \left(k_P v_{f,i} + k_I \int_0^{T_I} v_{f,i} \mathrm{d}s\right)(C_{s,i} - C_{c,i}) + G_i \cdot Occp_i, \tag{1f}$$

where zone $i \in \{1, 2, \ldots, m\}$, $T_{z,i}$ and $W_{z,i}$ are the air temperature and moisture content of zone i, respectively; $T_{z,j}$ means the air temperature of neighboring zone i. $C_{c,i}$ denotes the CO_2 concentration of zone i, $C_{s,i}$ represents the CO_2 concentration of supply air to zone i. $T_{s,i}$ and $W_{s,i}$ are the air temperature and moisture content leaving the indoor unit i, respectively; T_0 and W_0 are the outside air temperature and moisture content, respectively. $T_{d,i}$ is the air temperature leaving the dry-cooling region on the air side of the DX evaporator of indoor unit i, $T_{w,i}$ is the temperature of the DX evaporator wall in indoor unit i, $h_{s,i}$ is the enthalpy leaving the DX evaporator of indoor unit i. $v_{f,i}$ is the air volumetric flow rate of the supply fan i, $m_{r,i}$ is the mass flow rate of refrigerant to the indoor unit i. $h_{r1,i}$ and $h_{r2,i}$ are the enthalpies of refrigerant at the DX evaporator inlet and outlet of indoor unit i, respectively. V_i is the volume of zone i; $V_{h1,i}$ and $V_{h2,i}$ are the air side volumes in the dry-cooling region and wet-cooling region on the air side of the DX evaporator of indoor unit i, respectively. $C_{w,i}$, $\rho_{w,i}$ and $V_{w,i}$ are the specific heat of air, density of moist air and volume of the DX evaporator wall of indoor unit i, respectively. $\alpha_{dc,i}$ and $\alpha_{wc,i}$ are the heat transfer coefficients between air and the evaporator wall in the dry-cooling region and wet-cooling region of indoor unit i, respectively. $A_{1,i}$ and $A_{2,i}$ are the heat transfer areas in the dry-cooling region and wet-cooling region on the DX evaporator of indoor unit i, respectively, which are time-varying uncertainty and bounded parameters. $Occp_i$ is the number of occupants of zone i, G_i is amount of CO_2 emission rate of people at zone i. k_P and k_I are the parameter of the PI controller.

$R_{ij} = R_{ji}$ is the thermal resistance of the wall between zone i and j, R_i is the thermal resistance of the wall between zone i and the outside. If R_{ij} and R_i are not known from design specifications, they can

be obtained via model identification [31, 32]. T_{mix} and W_{mix} are the mixed air temperature and mixed moisture content before each DX evaporator cooling coil, respectively. The mixed air temperature and moisture content are calculated as follows:

$$T_{mix} = (1-\delta)T_0 + \delta\frac{\sum_{i=1}^{m} v_{f,i}T_{z,i}}{\sum_{i=1}^{m} v_{f,i}},\ W_{mix} = (1-\delta)W_0 + \delta\frac{\sum_{i=1}^{m} v_{f,i}W_{z,i}}{\sum_{i=1}^{m} v_{f,i}}, \tag{2}$$

where δ is the mixing ratio between the outside air and return air. It is assumed that the return air temperature and moisture content are the weighted sums of the zone temperatures and moisture contents with weights, being the air flow rate of supply air to the corresponding zones. The return air is not recirculated when $\delta = 0$, and no outside fresh air is used when $\delta = 1$. δ can be employed to save energy through recirculation but it has to be less than one to guarantee minimal outdoor fresh air delivered to the rooms. Note that the first equation of (2) is taken from [33]. It is assumed that the the mixed moisture content has a similar description in the second equation of (2). The airside convective heat transfer coefficients for the louvre-finned evaporator under both dry-cooling and wet-cooling regions on the air side of the evaporator i are calculated as follows [34]:

$$\alpha_{dc,i} = j_{dc}\rho v_{a,i}\frac{C_a}{Pr^{\frac{2}{3}}},\ \alpha_{wc,i} = j_{wc}\rho v_{a,i}\frac{C_a}{Pr^{\frac{2}{3}}},\ i = 1, 2, \ldots, m, \tag{3}$$

where Pr is the Prandtl number, j_{dc} and j_{wc} are the Colburn factors in the cooling mode. The air velocity $v_{a,i}$ is described as follows:

$$v_{a,i} = \frac{v_{f,i} - \varepsilon_i}{d_i},\ i = 1, 2, \ldots, m,$$

where d_i (m^2) is the cross-sectional area of zone i, ε_i is the non-desired air velocity through the door or window to pass in and out of the air to zone i, $v_{a,i}$ is the indoor air velocity of room i.

The above models (1a)-(1e) without considering outside air temperature and humidity entering into system for a single room were first built in [35]. The above models (1a)-(1f), absorbing CO_2 by an independent PSA box for a single room, were built in [11]. The above models (1a)-(1f) for a single room, absorbing CO_2 by using a PI controller based on a supply fan, were built in [12]. On the right-hand side of (1a), the first term denotes the heat transfer between zone i and all neighbours of zone i; the second term means the heat transfer between zone i and the outside wall. The PI controller in the equation (1f) is designed based on the air volumetric flow rate of the supply fan. It can be used for controlling the indoor CO2 concentration. In addition, the PI controller has the potential of reducing the complexity of computation and the cost of hardware.

Remark 1: Higher-order resistance-capacitance (RC) models were developed in [14, 16]. For simplicity, we only consider the first-order RC model in this paper. Though the higher-order RC models maybe more accurate than the first-order model, it is more difficult to use the current methods to solve the distributed control problem. Most existing works to solve the distributed control problem assume that interaction terms are either disturbances or negligible. We will study the distributed control problem of the higher-order RC models in the future.

Remark 2: The building DX A/C system's cooling and pollutant loads can be expressed in [12] and used as measurement information for an open loop controller in the upper optimization. The building loads are affected by some parameters (such as T_0, W_0, $Q_{rad,i}$, $Occp_i$, internal heat gain $Q_{int,i}$ and moisture ventilation load $M_{int,i}$). The prediction of these parameters can be obtained through a weather forecast station, historical data and schedules. Though the multi-zone buildings' cooling and pollutant loads cannot be accurately predicted, the designed AHDC strategy in the next section includes the DMPC controllers that are capable of handling the prediction errors.

To make the ME A/C system cooperatively control multi-zones' thermal comfort and air quality, we suppose that the ME A/C system is equipped with a communication network based on wireless communication. In this network, they can share information (e.g., $T_{z,i}$, $W_{z,i}$ and $C_{c,i}$) with one another, which is shown in Fig. 1. The information flow between them is modelled as a network graph $\mathcal{G} = (\mathcal{V}, \vartheta, \mathcal{A})$, where

$\mathcal{V} = \{1, 2, \ldots, m\}$ is the index set of different rooms and zones of the ME A/C system, $\vartheta \subset \mathcal{V} \times \mathcal{V}$ is the edge set of ordered pairs of the ME A/C system, and $\mathcal{A} = [a_{ij}] \in \mathbb{R}^{m \times m}$ is the adjacency matrix with entries $a_{ij} = 1$ or $a_{ij} = 0$. If the ME A/C subsystem i can receive information from the ME A/C subsystem j, then $(j, i) \in \vartheta$, $a_{ij} = 1$ and the ME A/C subsystem j is called the network neighbor of the ME A/C subsystem i, denoted by $j \in \mathcal{V}_i$, where $\mathcal{V}_i = \{j \in \mathcal{V} | a_{ij} = 1\}$. If the ME A/C subsystem i cannot have access to the information of the ME A/C subsystem j, then $(j, i) \notin \vartheta$, $a_{ij} = 0$ and $j \notin \mathcal{V}_i$. Self-connection is not considered for $\mathcal{G}$, i.e., $a_{ii} = 0$, $\forall i \in \mathcal{V}$. A graph $\mathcal{G}$ is undirected if $a_{ij} = a_{ji}$ for any $i, j \in \mathcal{V}$. In this paper, the network graph $\mathcal{G} = (\mathcal{V}, \vartheta, \mathcal{A})$ of the ME A/C system is assumed to be undirected and connected [36].

All the DX units of the ME A/C system adjust their comfort levels adaptively by acquiring the adjacent information. The neighbors of each DX unit can be defined in many different ways. In this paper, the following way is based on the effect of thermal resistance and is defined as follows:

$$\mathcal{V}_i = \{j : |R_{ij}| < \varepsilon_0, i \neq j\}, \tag{4}$$

where the parameter ε_0 is a predefined threshold, $\mathcal{V}_i$ is the set of neighbors of room i.

The system dynamic equations (1) can be written as equations of the following:

$$\dot{x}_i = f_i(x_i, x_{-i}, u_i, \omega_i), \ i = 1, 2, \ldots, m, \tag{5}$$

where the vector denoted as $x_i \triangleq [h_{s,i}, T_{z,i}, T_{d,i}, T_{w,i}, W_{z,i}, C_{c,i}]^T$ is the state of the subsystem S_i; $u_i = [v_{f,i}, m_{r,i}]^T$ are the constrained control signals; $\omega_i \triangleq [Q_{load,i}, M_{load,i}, C_{load,i}]^T$ represent the load variables of room i; and x_{-i} concatenate the states of all subsystems S_j ($j \in \mathcal{V}$) of the subsystem S_i, i.e., $x_{-i} = (x_1, \ldots, x_{i-1}, x_{i+1}, \ldots, x_m)$. The functions $f_i(x_i, x_{-i}, u_i, \omega_i)$ ($i = 1, 2, \ldots, m$) are defined as follows:

$$f_i(x_i, x_{-i}, u_i, \omega_i) = \begin{bmatrix} \frac{\alpha_{wc,i} A_{2,i} (T_{w,i} - \frac{T_{d,i} + T_{s,i}}{2}) + h_{fg} \rho v_{f,i} (W_{mix} - \frac{h_{s,i} - C_a T_{s,i}}{h_{fg}}) + C_a \rho v_{f,i} (T_{d,i} - T_{s,i})}{\rho V_{h2,i}} \\ \frac{\sum_{j=1}^{m} \frac{T_{z,j} - T_{z,i}}{R_{ij}} + \frac{T_0 - T_{z,i}}{R_i} + C_a \rho v_{f,i} (T_{s,i} - T_{z,i}) + Q_{load,i}}{C_a \rho V_i} \\ \frac{C_a \rho v_{f,i} (T_{mix} - T_{d,i}) + \alpha_{dc,i} A_{1,i} (T_{w,i} - \frac{T_{mix} + T_{d,i}}{2})}{C_a \rho V_{h1,i}} \\ \frac{\alpha_{dc,i} A_{1,i} (\frac{T_{mix} + T_{d,i}}{2} - T_{w,i}) + \alpha_{wc,i} A_{2,i} (\frac{T_{d,i} + T_{s,i}}{2} - T_{w,i}) - (h_{r2,i} - h_{r1,i}) m_{r,i}}{C_{w,i} \rho_{w,i} V_{w,i}} \\ \frac{\rho v_{f,i} (\frac{h_{s,i} - C_a T_{s,i}}{h_{fg}} - W_{z,i}) + M_{load,i}}{\rho V_i} \\ \frac{(k_P v_{f,i} + k_I \int_0^{T_I} v_{f,i} \mathrm{d}s)(C_{s,i} - C_{c,i}) + G_i \cdot Occp_i}{V_i} \end{bmatrix}. \tag{6}$$

2.3. Simplified energy models of the ME A/C system

The power consumers of the multi-zone building ME A/C system include the dampers, condenser fan, compressor and DX cooling coils. The power to drive the dampers is assumed to be negligible. The condenser fan power P_{con} is approximated as a second-order polynomial function of the total mass flow rate of refrigerant ($m_r = \sum_{i=1}^{m} m_{r,i}$) driven by the fan

$$P_{con} = c_0 + c_1 m_r + c_2 m_r^2, \tag{7}$$

where c_0, c_1 and c_2 are the parameters to be identified by curve-fitting of experimental data in [37].

The power consumption of the evaporator fans P_{eva} based on the energy conservation law is expressed as follows:

$$\begin{aligned} P_{eva} = \sum_{i=1}^{m} (a_0 + a_1 v_{f,i}, + a_2 v_{f,i}^2 + a_3 T_{s,i} + a_4 T_{s,i}^2 + a_5 Q_{c,i} + a_6 Q_{c,i}^2 + a_7 v_{f,i} T_{s,i} + \\ a_8 v_{f,i} Q_{c,i} + a_9 T_{s,i} Q_{c,i}), \end{aligned} \tag{8}$$

where the coefficients a_i ($i = 0, 1, \ldots, 9$) are constant and can be determined by curve-fitting of experimental data in [37]. $Q_{c,i}$ is the summation of the sensible and latent heat loads in room i.

The power consumption of the compressor P_{comp} is determined by [5]:

$$P_{comp} = \sum_{i=1}^{m} \frac{m_{r,i}(h_{r2,i} - h_{r1,i})}{\overline{\eta}}, \tag{9}$$

where $\overline{\eta}$ is the combined total efficiency of the compressor (known parameters).

The total electric power consumption P_{tot} of the multi-zone building ME A/C system at time t then is calculated as

$$P_{tot} = P_{con} + P_{eva} + P_{comp}. \tag{10}$$

2.4. PMV index

The PMV index was proposed by Fanger [38] and is used as a thermal comfort indicator. Fanger's index quantifies thermal sensation experienced by numerous people. The sensation is represented by a scale ranging from -3 (cold) to +3 (hot). The PMV index can be determined by personal and environmental factors. The personal factors consist of metabolic rate M_r (W/m^2) and clothing insulating I_{cl} (m$^{2\circ}$C/W). The environmental factors comprise air temperature T_z, air humidity (or moisture content) W_z, air velocity v_a and mean radiant temperature T_r. The function of the conventional PMV index for a single zone is depicted by

$$PMV = g(T_z, W_z, v_a, M_r, I_{cl}, T_r), \tag{11}$$

where the specific expression can be described in [38].

Conventionally, the PMV index is an indicator of indoor air temperature and humidity [6, 9, 39, 40]. The CO_2 concentration, air temperature and humidity have become three major indicators of thermal comfort and IAQ. The separate control of the PMV index and CO_2 concentration was studied in [4, 41]. However, three coupling effects of indoor air temperature, humidity and CO_2 concentration cannot be ignored in many cases. In fact, indoor humidity was correlated with CO_2 concentration according to measurement results reported in [42]. Furthermore, the experimental investigation [43] suggested that the value of the PMV index was affected by control of the indoor CO_2 concentration. To our best knowledge, very little work exists in the literature that proposes mathematical equations among the indoor air temperature, relative humidity and CO_2 concentration. We propose simplified mathematical equations such that the PMV index includes indoor thermal comfort and CO_2 concentration in this study.

M_r is the rate of metabolism, which denotes the amount of energy used by a person per unit of time. From the study of [44], the metabolic rate is directly related to a person's energy output, which can be expressed by calorie output per hour and a body's surface area

$$M_r = K_p/S_p, \tag{12}$$

where K_p denoting a person's heat output per hour is the calorie of 1L of oxygen consumed, S_p is the body surface area and can be expressed as [44]

$$S_p = 0.007184H^{0.725}W^{0.425}, \tag{13}$$

where H and W are the height (cm) and weight (kg) of a person, respectively. For 1L oxygen consumed, we have [44]

$$\begin{cases} 1L \text{ O}_2 \text{ consumed} = a + b + c = 1, \\ 1L \text{ CO}_2 \text{ produced} = R = a + 0.802b + 0.718c, \\ K_p = 5.047a + 4.463b + 4.735c, \end{cases} \tag{14}$$

where a is the carbohydrate, b denotes the protein and c represents the fat which is obtained by 1L of oxygen metabolizing. The third equation of (14) can be reduced to the following one

$$K_p = 3.9 \times \text{L O}_2 \text{ used} + 1.1 \times \text{L CO}_2 \text{ produced} = 3.9 * V_o + 1.1 * G, \tag{15}$$

where V_o is the amount of oxygen consumed per unit of hour (l/h). This equation was widely cited and can be used for estimating the energy expenditure, oxygen consumed and CO_2 produced [45, 46, 47].

Under normal conditions, when a body is at rest and in nutritional equilibrium, the global respiratory ratio is $m_{\mathrm{CO}_2}/m_{\mathrm{O}_2} = 0.83$ as reported in [48]. Since this study investigates thermal comfort and IAQ of offices, we assume $G/V_o = 0.83$. One can then obtain

$$K_p = \frac{481.3}{83} * G, \tag{16}$$

According to (12), one can obtain that the metabolic rate in human metabolism of room i denoted by M_{r_i} has the following equation

$$M_{r_i} = \frac{481.3}{83 S_{p_i}} * G_i, \ i = 1, 2, \ldots, m. \tag{17}$$

where S_{p_i} is the body surface area of room i.

Based on the equations (17) and (1f), M_{r_i} under a steady state of the CO_2 concentration in room i can be expressed by

$$M_{r_i} = \frac{481.3}{83 S_{p_i} \cdot Occp_i}(k_P v_{f,i} + k_I \int_0^{T_I} v_{f,i} \mathrm{d}s)(C_{c,i} - C_{s,i}), \ i = 1, 2, \ldots, m. \tag{18}$$

This equation implies that the metabolic rate can reflect indoor CO_2 concentration produced.

Then the PMV_i index is the function of the following variables:

$$PMV_i = g_i(T_{z,i}, W_{z,i}, C_{c,i}, v_{f,i}, I_{cl}, T_r), \ i = 1, 2, \ldots, m. \tag{19}$$

It can be noted from this equation that the PMV index can be used as an indicator of thermal comfort and IAQ of room i.

The equation (18) represents a condition under which the steady states of the system are reached, i.e., there is a relationship between the metabolic rate, CO_2 concentration and air volumetric flow rate at steady states. In fact, for the same activity of a person, his respiratory change is determined by the indoor air temperature or/and humidity. A person's metabolic rate is directly reflected by a respiratory change. The high or low temperature or/and humidity can cause the occupant to breathe out either more or less CO_2, thus the indoor air temperature or/and humidity can influence the metabolic rate. On the other hand, the air volumetric flow rate determines the indoor air temperature and humidity and their eventual steady states. Therefore, the air volumetric flow rate is indirectly related to the metabolic rate.

Remark 3: Most previous works used the PMV index as a thermal comfort indicator. From function (19), it can be seen that the modified PMV index has been extended and used as an indicator of both thermal comfort and IAQ in the normal office buildings.

2.5. Constraints

The multi-zone building ME A/C system is subject to thermal comfort and IAQ constraints, and cooling operational constraints are defined as below.

(C1) $\mathrm{PMV}_i \in [\underline{\mathrm{PMV}}_i, \overline{\mathrm{PMV}}_i], \ i = 1, 2, \ldots, m.$ Each room's thermal comfort and IAQ are within the comfort ranges.

(C2) $\delta \in [\underline{\delta}, \overline{\delta})$. The upper and lower bounds limit the ratio of the outside air entering the system.

(C3) $T_{z,i} \in [\underline{T}_{z,i}, \overline{T}_{z,i}], \ W_{z,i} \in [\underline{W}_{z,i}, \overline{W}_{z,i}], \ C_{c,i} \in [\underline{C}_{c,i}, \overline{C}_{c,i}], \ i = 1, 2, \ldots, m.$ Each room's air temperature, moisture content and CO_2 concentration are within the required ranges for occupants in the cooling mode.

(C4) $T_{s,i} \in [\underline{T}_{s,i}, \overline{T}_{s,i}], \ W_{s,i} \in [\underline{W}_{s,i}, \overline{W}_{s,i}], \ i = 1, 2, \ldots, m.$ The bounds of the air temperature and moisture leaving the DX evaporator are limited because of the physical characteristics of the coils and the air cooling coils of the DX evaporators. Besides, the upper bounds $\overline{T}_{s,i}$ and $\overline{W}_{s,i}$ are less than $T_{z,i}$ and $W_{z,i}$

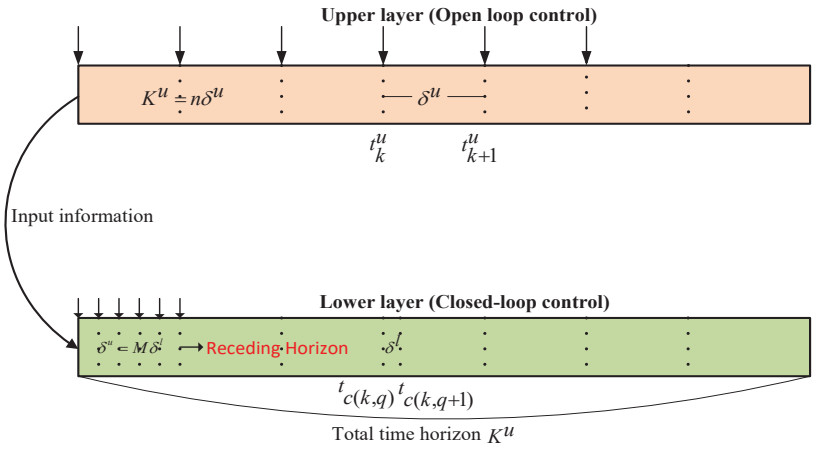

Figure 2: Simplified schematic of two-layer time index.

respectively since they are used for cooling and dehumidifying of each room. The bound of the air enthalpy $h_{s,i}$ satisfies: $h_{s,i} \in [C_z\underline{T}_{s,i} + h_{fg}\underline{W}_{s,i}, C_a\overline{T}_{s,i} + h_{fg}\overline{W}_{s,i}]$.

(C5) $\sum_{i=1}^{m} v_{f,i}T_{s,i} \leq \sum_{i=1}^{m} v_{f,i}T_{mix}$, $\sum_{i=1}^{m} v_{f,i}W_{s,i} \leq \sum_{i=1}^{m} v_{f,i}W_{mix}$. The mixed air temperature and moisture content after each DX evaporator can only decrease.

(C6) $T_{d,i} \leq T_{mix}$, $T_{w,i} \leq T_{d,i}$, $W_{s,i} \leq W_{mix}$, $i = 1, 2, \ldots, m$. Air temperature and moisture content after each DX dry-cooling and wet-cooling regions can only decrease, respectively.

(C7) $v_{f,i} \in [\underline{v}_{f,i}, \overline{v}_{f,i}]$, $m_{r,i} \in [\underline{m}_{r,i}, \overline{m}_{r,i}]$, $i = 1, 2, \ldots, m$. The upper bounds of the air volumetric flow rate $\overline{v}_{f,i}$ and the mass flow rate of refrigerant $\overline{m}_{r,i}$ of each room are limited by the physical characteristics of the multi-zone building ME A/C system. The lower bounds $\underline{v}_{f,i} > 0$ and $\underline{m}_{r,i} > 0$ are matched minimum operation and ventilation demands.

The constraints in (C1)-(C7) are compactly written as

$$x_i \in \mathbb{X},\ u_i \in \mathbb{U},\ h_{1,i}(x_i, u_i) \leq 0,\ h_{2,i}(x_i) \leq 0 \text{ and } PMV_i \in \mathbb{F},\ i = 1, 2, \ldots, m. \tag{20}$$

where $\mathbb{X}$, $\mathbb{U}$, $\mathbb{P}$ and $\mathbb{F}$ are bounded sets, $h_{1,i}(x_i, u_i)$ and $h_{2,i}(x_i)$ can be written as functions of the state and input variables, where they correspond to constraints in (C5) and (C6).

3. Controller design

To facilitate the description of the proposed AHDC strategy for the nonlinear systems (5), the notation ^{u} will be used for the upper layer control and ^{l} will be used for the lower layer DMPC. We will abbreviate the upper layer open loop controller to UOPC while the lower layer DMPC as LDMPC for short. t_k^u denotes the sampling time instant of the UOPC and t_k^l represents that of the lower level DMPC; assume $c(k, q) \triangleq kM+q$, where M is a positive integer number corresponding to the number of sampling instants of the LDMPC between two sampling instants of the UOPC; $t_k^u \triangleq t_{c(k,0)}^l$; $\delta^u \triangleq t_{k+1}^u - t_k^u$ and $\delta^l \triangleq t_{k+1}^l - t_k^l$ denote the sampling period of the UOPC and LDMPC, respectively; $\delta^u = M\delta^l$. T^l denotes the prediction horizon of the LDMPC, which satisfies $\delta^u \geq T^l$.

Throughout the rest of this paper, we denote the long-term scale horizon as $[0, K^u]$, and $K^u = n\delta^u$ ($n \in N^+$). Fig. 2 shows the time index of the two layers and that the upper layer sends information to the lower layer.

3.1. Upper level: steady state optimization problem

In reality, each zone has desired air temperature, humidity and CO_2 concentration, the reference points of which are determined by users. The objective of the upper layer considered in this paper is to minimize the

total electricity bills in the building, which reflect demand and energy costs under the TOU rate structure, and to generate optimal reference points of air temperature, humidity and CO_2 concentration for each zone for the lower layer. More specifically, we consider the following centralized steady-state optimization problem:

$$X^*(t_k^u) = \arg\min_{x(t_k^u),u(t_k^u)} \Big(\underbrace{\sum_{i=1}^{m}\Big[w_1 \sum_{k=1}^{n}\big(E_c(t_k^u)P_{tot,i}(t_k^u)\delta^u\big)}_{\text{energy cost}} + \underbrace{w_2(D_c(t_k^u)\max_{1\le k\le n}\{P_{tot,i}(t_k^u)\})\Big]}_{\text{demand cost}} \Big), \tag{21a}$$

subject to the following constraints:

$$f_i(x_i(t_k^u), x_{-i}(t_k^u), u_i(t_k^u), \omega_i(t_k^u)) = 0,\ i = 1, 2, \ldots, m, \tag{21b}$$

$$|PMV_i(t_k^u)| \le \alpha,\ i = 1, 2, \ldots, m, \tag{21c}$$

$$x_i(t_k^u) \in \mathbb{X}_i,\ u_i(t_k^u) \in \mathbb{U}_i,\ h_{1,i}(x_i(t_k^u), u_i(t_k^u)) \le 0,\ h_{2,i}(x_i(t_k^u)) \le 0,\ i = 1, 2, \ldots, m, \tag{21d}$$

where $t_k^u \in [0, K^u]$, $x(t_k^u) = [x_1(t_k^u), \ldots, x_m(t_k^u)]^T$ is the system state, $u(t_k^u) = [u_1(t_k^u), \ldots, u_m(t_k^u)]^T$ is the control input. The total energy consumption P_{tot} is expressed in (10) and the PMV function is described in (19). Constant α is the comfort bounded of the value of the PMV index. $E_c(t_k^u)$ is the TOU electricity rate at time step t_k^u, and $D_c(t_k^u)$ is the demand charge rate at time step t_k^u. w_i $(i = 1, 2)$ denote the positive weighting factors and $f_i(x_i(t_k^u), x_{-i}(t_k^u), u_i(t_k^u), \omega_i(t_k^u))$ are defined in (6). $X^*(t_k^u)$ is a global optimal solution of the optimization problem (21).

Before investigating the distributed steady state optimization problem, we make an assumption on the system model.

Assumption 1. The optimal problem (21) admits a solution, of which the steady state of temperature, humidity and CO_2 concentration for each zone are approximately the same.

This assumption is valid in many practical situations where the different zones serve the same functions and purposes; for example in an office environment, the comfort requirements are subject to the same standards, ambient conditions and energy regulatory and pricing structure and are therefore normally the same.

This assumption may not hold in cases where buildings have different functional zones such as offices and ancillary equipment spaces. The similar algorithms can be extended to the cases when different functional zones can be grouped into homogeneous ones.

Secondly, under a steady state, the total heat gain from neighboring zones is sometimes less dominant compared with that from the outside plus the indoor heat gain in every zone. As reported in [12], the TOU rate structure is also the main factor to dominate the steady state optimization solutions. Therefore, in the optimization problem (21), we can ignore the interacting terms $\Sigma_{j=1,j\neq i}^{m} \frac{T_{z,j}-T_{z,i}}{R_{ij}}$ in (1a) or $\Sigma_{j=1,j\neq i}^{m} \frac{T_{z,j}-T_{z,i}}{R_{ij}}$ in (21b). Thereby, a simplified optimization problem (22) is considered for one zone i only as follows:

$$X_i^r(t_k^u) = \arg\min_{x_i(t_k^u),u_i(t_k^u)} \Big(\underbrace{w_1 \sum_{k=1}^{n}\big(E_c(t_k^u)P_{tot,i}(t_k^u)\delta^u\big)}_{\text{energy cost}} + \underbrace{w_2(D_c(t_k^u)\max_{1\le k\le n}\{P_{tot,i}(t_k^u)\})}_{\text{demand cost}} \Big), \tag{22a}$$

subject to the following constraints:

$$\widetilde{f}_i(x_i(t_k^u), u_i(t_k^u), \omega_i(t_k^u)) = 0, \tag{22b}$$

$$|PMV_i(t_k^u)| \le \alpha, \tag{22c}$$

$$x_i(t_k^u) \in \mathbb{X}_i,\ u_i(t_k^u) \in \mathbb{U}_i,\ h_{1,i}(x_i(t_k^u), u_i(t_k^u)) \le 0,\ h_{2,i}(x_i(t_k^u)) \le 0, \tag{22d}$$

where $t_k^u \in [0, K^u]$, $X_i^r(t_k^u)$ is a local optimal solution, and i means that the optimization problem (22) only needs the measurement information of room i. Here, $\widetilde{f}_i(x_i, u_i, \omega_i)$ is described by

$$\widetilde{f}_i(x_i,u_i,\omega_i) = \begin{bmatrix} \frac{\alpha_{wc,i}A_{2,i}(T_{w,i}-\frac{T_{d,i}+T_{s,i}}{2})+h_{fg}\rho v_{f,i}(W_{mix}-\frac{h_{s,i}-C_aT_{s,i}}{h_{fg}})+C_a\rho v_{f,i}(T_{d,i}-T_{s,i})}{\rho V_{h2,i}} \\ \frac{\frac{T_0-T_{z,i}}{R_i}+C_a\rho v_{f,i}(T_{s,i}-T_{z,i})+Q_{load,i}}{C_a\rho V_i} \\ \frac{C_a\rho v_{f,i}(T_{mix}-T_{d,i})+\alpha_{dc,i}A_{1,i}(T_{w,i}-\frac{T_{mix}+T_{d,i}}{2})}{C_a\rho V_{h1,i}} \\ \frac{\alpha_{dc,i}A_{1,i}(\frac{T_{mix}+T_{d,i}}{2}-T_{w,i})+\alpha_{wc,i}A_{2,i}(\frac{T_{d,i}+T_{s,i}}{2}-T_{w,i})-(h_{r2,i}-h_{r1,i})m_{r,i}}{C_{w,i}\rho_{w,i}V_{w,i}} \\ \frac{\rho v_{f,i}(\frac{h_{s,i}-C_aT_{s,i}}{h_{fg}}-W_{z,i})+M_{load,i}}{\rho V_i} \\ \frac{(k_P v_{f,i}+k_I\int_0^{T_I} v_{f,i}\mathrm{d}s)(C_{s,i}-C_{c,i})+G_i\cdot Occp_i}{V_i} \end{bmatrix}. \tag{23}$$

We have five important remarks for the optimization problem (22).

- In (22a), the term regarding the end-user services contains two parts, i.e., the energy cost of the multi-zone building ME A/C system given by $\sum_{k=1}^{n}\left[E_c(t_k^u)P_{tot,i}(t_k^u)\delta^u\right]$ (weighted by w_1) aims to minimise energy cost, the peak demand $D_c(t_k^u)\max_{1\le k\le n}\left\{P_{tot,i}(t_k^u)\right\}$ (weighted by w_2) aims to reduce demand cost.

- The weighting factors w_1 and w_2, which are determined by users, are to balance the two objectives. Specifically, if preferring more demand reduction, they can increase w_2 and decrease w_1 and vice versa.

- It can be seen in (22a) that the energy and demand rates $E_c(t_k^u)$ and $D_c(t_k^u)$ depend on the TOU. The rate structures are determined by utilities for various types of customers. For some rate plans, customers have the flexibility to choose peak periods so that they can save cost by optimizing energy use during specific time periods.

- This steady state optimization problem is different from our previous work [11, 12]. In [11], an open loop optimal control algorithm was proposed to minimize energy consumption by setting temperature, humidity and CO_2 concentration. In [12], an open loop steady state optimal control algorithm is autonomously and adaptively setting optimal temperature, humidity and CO_2 concentration references, which could be time-varying to minimize energy cost and the PMV index. This study proposes an open loop optimal controller that minimizes the energy and demand charge costs under the PMV index within acceptable ranges. It reaches the same conclusions as [12] in scheduling the reference setpoints. On the other hand, this study considers a DR action, which can further improve energy efficiency and reduce energy cost, it is different from our previous work [11, 12] without consideration of that action.

- The optimal solution applies to one zone, and the resulting reference setpoints are then communicated to the whole network through connecting neighbors. Therefore, the scheduling is implementable in a distributed manner.

The ADSMS is a hierarchical distributed way that aims at achieving energy and cost savings in ME A/C operations without compromising occupancy comfort levels. The information communication for the simplified ADSMS is illustrated in Fig. 3. The idea here is to consider comfort as a service for occupants. The zones (using zone modules (ZMs)) are customers seeking this service (called token), and a distribution system operator (DSO) is the service provider (called provider). There are four steps in the ADSMS that are explained in the following:

1) Master: The DSO collects one zone's measurement information (cooling and pollutant loads, weather and occupancy), then computes and transmits optimal reference signals to this zone by a communication network.

2) Slave: The neighboring zones receive communication information using numerous ZMs from the driving system. Then neighbouring zones then communicate to whole zones through connecting neighbors.

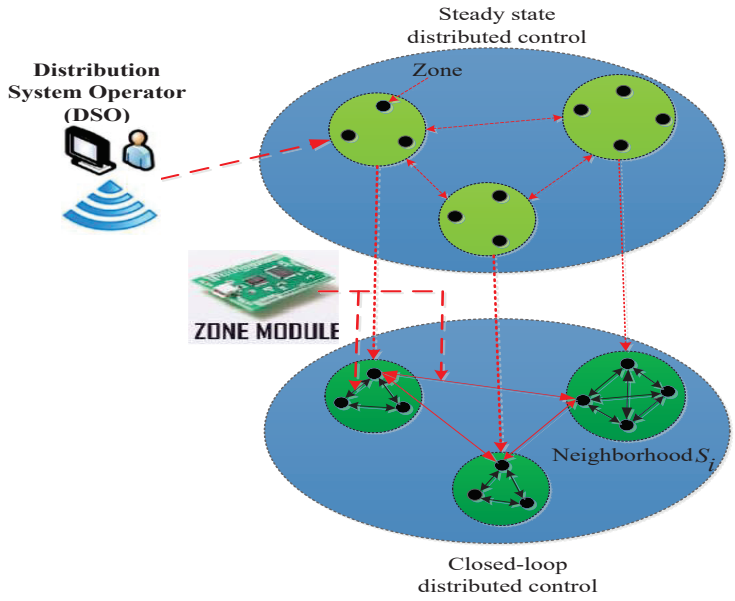

Figure 3: Autonomous demand-side management scheduling architecture.

3) Token requests: The main aim of the ZM is to run an MPC using forecast information (weather condition, occupancy and cooling and pollutant loads) plus sensor readings (temperature and humidity, thermostat and CO_2 sensors) to compute the minimal energy consumption and cost required without breaching comfort ranges.

4) Coordination: After each room receives communication information, each DX unit employs a DMPC algorithm to optimise the transient process of reaching thermal comfort and satisfying IAQ demands while minimize energy consumption and costs.

Remark 4: For ease of implementation, the min-max problem in (22a) is converted into the standard nonlinear programming described below so that it can be conveniently solved by the Matlab built-in functions. A new variable z_P is introduced to represent the peak demand of the day for zone i only as follows:

$$z_{P,i} = \max_{1\le k\le n}\{P_{tot,i}(t_k^u)\}. \tag{24}$$

By simplifying the objective to the form in (25), the optimization problem in (22a) can be rewritten as

$$\min \ \Big(w_1 \sum_{k=1}^{n} E_c(t_k^u) P_{tot,i}(t_k^u)\delta^u + w_2 D_c(t_k^u) z_{P,i}\Big). \tag{25}$$

3.2. Lower level: DMPC

To conclude, the goal of the lower layer is to design the tracking rule $u(t_k^u)$ in a distributed way so that each subsystem of (5) can reach its steady states according to the changing environment during the day.

The UOPC transmits the reference signals, $x^r(s;t_k^u) = [x_1^r(s;t_k^u),\dots,x_m^r(s;t_k^u)]^T, u^r(s;t_k^u) = [u_1^r(s;t_k^u), \dots, u_m^r(s;t_k^u)]^T, T_{s,i}^r(s;t_k^u), \delta(s;t_k^u)$, to the LDMPC for $s \in [t_k^u, t_{(k+1)}^u), i = 1,2,\dots,m$. Here, $x^r(t_k^u) \triangleq x^r(t_k^u;t_k^u)$. In the lower layer, the DMPC controllers are designed to steer for the multi-zone building ME A/C system to track the trajectory references calculated by the upper layer. The linearized dynamic subsystem S_i for the nonlinear systems (5) around the trajectory references at sampling time instant $t_{c(k,q)}^l$ can be written as given below. In (26), the interacting terms in non-neighboring zone are ignored because of our definition of neighbors in (4).

$$\begin{cases} \delta\dot{x}_i(s) = A_{ii}(t_{c(k,q)}^l)\delta x_i(s) + \sum_{j\in\mathcal{V}_i} A_{ij}(t_{c(k,q)}^l)\delta x_j(s) + B_i(t_{c(k,q)}^l)\delta u_i(s), \\ y_i(s) = C_{ii}\delta x_i(s) + y_i^r(s), \quad s \in [t_{c(k,q)}^l, t_{c(k,q)}^l + T^l), \ i = 1,2,\dots,m, \end{cases} \tag{26}$$

where $A_{ii}(t^l_{c(k,q)}) = \frac{\partial f_i}{\partial x_i}(x^r_i(t^l_{c(k,q)}), u^r_i(t^l_{c(k,q)}))$, $A_{ij}(t^l_{c(k,q)}) = \frac{\partial f_i}{\partial x_j}(x^r_j(t^l_{c(k,q)}), u^r_j(t^l_{c(k,q)}))$, $B_i(t^l_{c(k,q)}) = \frac{\partial f_i}{\partial u_i}(x^r_i(t^l_{c(k,q)}), u^r_i(t^l_{c(k,q)}))$ for $j \in \mathcal{V}_i$. $\delta x_i(s)$ and $\delta u_i(s)$ are the deviations of state and input from their trajectory references, respectively; $y_i = [T_{z,i}, W_{z,i}, C_{c,i}]^T$ are the original output variables; $y^r_i = [T^r_{z,i}, W^r_{z,i}, C^r_{c,i}]^T$ are the trajectory references in the lower layer, which are calculated in the upper layer.

The predicted subsystem S_i can be written as follows:

$$\begin{cases} \delta\dot{x}^p_i(s; t^l_{c(k,q)}) = A_{ii}(s; t^l_{c(k,q)})\delta x^p_i(s; t^l_{c(k,q)}) + \sum_{j\in\mathcal{V}_i} A_{ij}(t^l_{c(k,q)})\delta\widehat{x}_j(s; t^l_{c(k,q)}) + \\ \qquad\qquad B_i(s; t^l_{c(k,q)})\delta u^p_i(s; t^l_{c(k,q)}), \\ y^p_i(s; t^l_{c(k,q)}) = C_{ii}\delta x^p_i(s; t^l_{c(k,q)}) + y^r_i(s; t^l_{c(k,q)}),\ s \in [t^l_{c(k,q)}, t^l_{c(k,q)} + T^l),\ i = 1, 2, \ldots, m, \end{cases} \tag{27}$$

where $\delta x^p_i(s; t^l_{c(k,q)})$, $\delta u^p_i(s; t^l_{c(k,q)})$ and $y^p_i(s; t^l_{c(k,q)})$ are the predicted state, input and output trajectories at time step $t^l_{c(k,q)}$, $\delta\widehat{x}_j(s; t^l_{c(k,q)})$ is the assumed state sequence of S_i at time step $t^l_{c(k,q)}$.

The MPC algorithm is designed for the lower layer to minimize the optimization objective after reaching trajectory references as well as to handle building external disturbances and to compensate for the model mismatch. Let

$$\delta u^p_i(s; t^l_{c(k,q)}) = -\sum_{j\in\mathcal{V}_i} K_j(s; t^l_{c(k,q)})\delta\widehat{x}_j(s; t^l_{c(k,q)}) + v^p_i(s; t^l_{c(k,q)}),\ s \in [t^l_{c(k,q)}, t^l_{c(k,q)} + T^l), \tag{28}$$

where $i = 1, 2, \ldots, m$, $K_j(s; t^l_{c(k,q)})$ is the gain matrix from zone j, $v_i(s; t^l_{c(k,q)})$ is a new input variable for zone i, then (27) is converted to (29) as follows:

$$\begin{cases} \delta\dot{x}^p_i(s; t^l_{c(k,q)}) = A_{ii}(s; t^l_{c(k,q)})\delta x^p_i(s; t^l_{c(k,q)}) + B_i(t^l_{c(k,q)})v^p_i(s; t^l_{c(k,q)}), \\ y^p_i(s; t^l_{c(k,q)}) = C_{ii}\delta x^p_i(s; t^l_{c(k,q)}) + y^r_i(s; t^l_{c(k,q)}),\ s \in [t^l_{c(k,q)}, t^l_{c(k,q)} + T^l),\ i = 1, 2, \ldots, m. \end{cases} \tag{29}$$

Many standard approaches exist in [23, 25] for the system (29), which depends entirely on one zone i. In this paper, we are using the MPC strategy proposed by our previous work [12], then the proposed optimization objective is given by

$$\begin{aligned} \min_{v^p_i(s;t^l_{c(k,q)})} \overline{J}^l_i = \int_{t^l_{c(k,q)}}^{t^l_{c(k,q)}+T^l} & \left(\left\|y^p_i(s; t^l_{c(k,q)}) - y^r_i(s; t^l_{c(k,q)})\right\|^2_{Q_i} + \left\|v^p_i(s; t^l_{c(k,q)})\right\|^2_{R_i}\right)ds \\ & + \left\|y^p_i(t^l_{c(k,q)} + T^l; t^l_{c(k,q)}) - y^r_i(t^l_{c(k,q)} + T^l)\right\|^2_{P_i},\ i = 1, 2, \ldots, m, \end{aligned} \tag{30a}$$

subject to:

$$\delta\dot{x}^p_i(s; t^l_{c(k,q)}) = A_{ii}(s; t^l_{c(k,q)})\delta x^p_i(s; t^l_{c(k,q)}) + B_i(s; t^l_{c(k,q)})v^p_i(s; t^l_{c(k,q)}),\ i = 1, 2, \ldots, m, \tag{30b}$$

$$y^p_i(s; t^l_{c(k,q)}) = C_{ii}\delta x^p_i(s; t^l_{c(k,q)}) + y^r_i(s; t^l_{c(k,q)}),\ i = 1, 2, \ldots, m, \tag{30c}$$

$$x^p_i(s; t^l_{c(k,q)}) \in \mathbb{X},\ v^p_i(s; t^l_{c(k,q)}) \in \mathbb{V},\ i = 1, 2, \ldots, m, \tag{30d}$$

where $s \in [t^l_{c(k,q)}, t^l_{c(k,q)} + T^l)$, $\overline{J}^l_i$ is the lower layer objective function i, the controllers $\delta u^p_i(s; t^l_{c(k,q)})$ obtained are distributed. Q_i, R_i, P_i are the weighting matrix, $\mathbb{V}$ is a bounded set of the new input variable v_i. The convergence for the above finite horizon periodic MPC optimization problem (30) can be proved by the results in [49, 50].

The implementation strategy of the proposed AHDC algorithms for a multi-zone building ME A/C system can be summarized as follows:

The algorithm 1 in our previous work [12] is adopted to solve the upper layer distributed steady state optimization problem.

Algorithm: The lower layer DMPC algorithm can be given below.

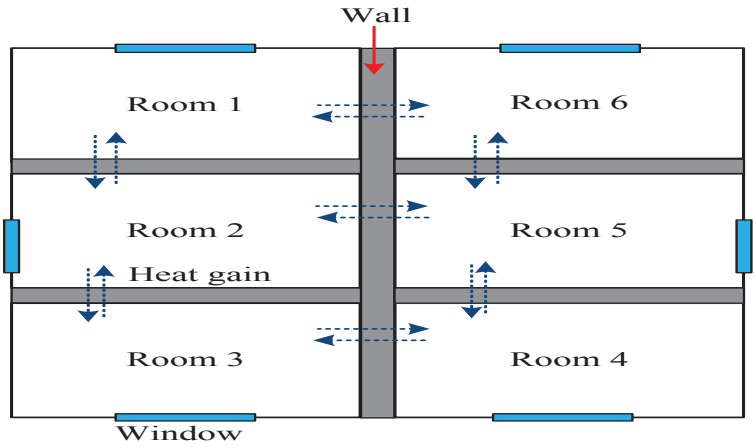

Figure 4: Schematic of six-rooms building with the thermal network for all zones and its surrounding walls.

1) At sampling time instant $t_k^u,\ k = 0, 1, \ldots, n$, UOPC receives each local neighbor's measurement information.

2) UOPC computes the state trajectory $x^r(s; t_k^u) = [x_1^r(s; t_k^u), \ldots, x_m^r(s; t_k^u)]^T,\ s \in [t_k^u, t_{k+1}^u)$ and its corresponding control input trajectory $u^r(s; t_k^u) = [s; u_1^r(t_k^u), \ldots, u_m^r(s; t_k^u)],\ s \in [t_k^u, t_{k+1}^u)$, which are transmitted to LDMPC, to obtain linearized systems (29).

3) At sampling time instant $t_{c(k,q)}^l$, LDMPCi receives the state measurement $x_i(s; t_{c(k,q)}^l)$ and $x_{-i}(s, t_{c(k,q)}^l)$ from its neighbors, gives an initial point $x_i(0)$ $(k = q = 0)$ and computes the optimal control input $v_i^*(s; t_{c(k,q)}^l)$ of the optimization problems (30) over the prediction horizon $[t_{c(k,q)}^l, t_{c(k,q)}^l + T^l]$.

4) The first solution $v_i^*(s; t_{c(k,q)}^l)$ is used through (28) to update $\delta u_i^p(s; t_{c(k,q)}^l)$ as the initial condition over the next prediction horizon $[t_{c(k,q+1)}^l, t_{c(k,q)}^l + \delta^l]$.

5) If $0 \leq q < M,\ q = q + 1$ and go to 3); else $k = k + 1,\ q = 0$ and go to 1).

4. Case study

In this section, a six-room model is considered to simulate the performance of the proposed AHDC strategy in special climate conditions in Cape Town, South Africa. The simulations are conducted during normal operation of an office building with normal occupancy. The six rooms are connected and the undirected graph is $\mathcal{G} = \{\mathcal{V}, \mathcal{A}\}$ where $\mathcal{V} = \{1, 2, 3, 4, 5, 6\}$ and $\varepsilon_0 = 5$. $R_{12} = R_{21} = R_{23} = R_{32} = R_{34} = R_{43} = R_{45} = R_{54} = R_{56} = R_{65} = R_{61} = R_{16} = 4 < \varepsilon_0$, $R_{13} = R_{31} = R_{24} = R_{42} = R_{35} = R_{53} = R_{46} = R_{64} = R_{51} = R_{15} = R_{62} = R_{26} = 8 > \varepsilon_0$, $R_{14} = R_{41} = R_{25} = R_{52} = R_{36} = R_{63} = 12 > \varepsilon_0$, then the neighbors of zone i are depicted in Table 1. As an illustrating example, Fig. 4 shows the schematic of a six-room building with the thermal network. It can be verified that the network is connected.

Table 1: The neighborhood definition of zones

Room (i)	Neighbors $(\mathcal{V}_i)$	Room (i)	Neighbors $(\mathcal{V}_i)$
1	2,6	2	1,3
3	2,4	4	3,5
5	4,6	6	5,1

4.1. Parameter selection

The volume of each room space is 77 m^3. The model parameters of the multi-zone building ME A/C system are given in Table 2. The coefficients of the power consumption models for the condenser (7) and

evaporators (8) are calibrated through the regression analysis of the available measured data in [37], which are shown in Table 3. It is assumed that the combined total efficiency of the compressor $\overline{\eta}$ is 0.85. Each room has a window with the area of 4 m^2. For the proposed AHDC strategy considered below, the system variable constraints are given by bounds in Table 4, and we constrain the value of each room's PMV index in the range of $[-0.5, 0.5]$ to ensure that the multi-zone building ME A/C system is able to control each room's thermal comfort and IAQ at the required levels for occupants. The weighting factors are defined as $w_1 = 1$, $w_2 = 1$. In our previous work [12], the simulation results demonstrated that the open loop optimal controller and the MPC scheme are not sensitive to the model parameters A_1 and A_2 of the single-zone DX A/C system within any ranges of $[aA_0, bA_0]$ where $0 \leq a, b \leq 1$ and $a \leq b$. This result can be extended to the multi-zone building ME A/C system. Hence, $A_{1,i} = 0.15A_{0,i}$ and $A_{2,i} = 0.85A_{0,i},\ i \in \mathcal{V}$ are chosen in this paper.

Table 2: Model parameters of the ME A/C system.

Notations	Values	Notations	Values
ρ	1.2 kg/m^3	h_{fg}	2450 kJ/kg
V_i	77 m^3	ε_{win}	0.45
V_{h1}	0.04 m^3	V_{h2}	0.16 m^3
k_{spl}	0.0251 kJ/m^3	C_a	1.005 kJ kg^{-1} $°C^{-1}$
$A_{0,i}$	22.07 m^3	R_i	15°C/kW

Table 3: Coefficients of energy models.

Notations	Values	Notations	Values
$a_0 = 900.5$	$a_1 = -8.1$	$a_2 = 6.18$	$a_3 = -0.15$
$a_4 = -4.61$	$a_5 = 0.02$	$a_6 = -0.2$	$a_7 = 0.01$
$a_8 = 0.12$	$a_9 = 0.09$	$c_0 = 138.1$	$c_1 = 0.52$
$c_2 = -2.3$			

Table 4: Values of system constraints.

Notations	Values	Notations	Values
$\overline{T}_{s,i}$	22 °C	$\underline{T}_{s,i}$	8 °C
$\overline{T}_{z,i}$	26 °C	$\underline{T}_{z,i}$	22 °C
$\overline{T}_{d,i}$	22 °C	$\underline{T}_{d,i}$	10 °C
$\overline{T}_{w,i}$	22 °C	$\underline{T}_{w,i}$	10 °C
$\overline{W}_{z,i}$	12.3/1000 kg/kg	$\underline{W}_{z,i}$	9.85/1000 kg/kg
$\overline{C}_{c,i}$	800 ppm	$\underline{C}_{c,i}$	650 ppm
$\overline{W}_{s,i}$	9.85/1000 kg/kg	$\underline{W}_{s,i}$	7.85/1000 kg/kg
$\overline{v}_{f,i}$	0.8 m^3/s	$\underline{v}_{f,i}$	0.05 m^3/s
$\overline{m}_{r,i}$	0.11 kg/s	$\underline{m}_{r,i}$	0.005 kg/s
$\overline{h}_{s,i}$	46.3 kJ/kg	$\underline{h}_{s,i}$	27.3 kJ/kg
α	0.5		

The simulation runs from 0:00 to 23:59. The environmental temperature and relative humidity information are obtained from a meteorological station located in Cape Town, South Africa. The outside air temperature and relative humidity profiles are plotted in Fig. 5(a). The predicted solar radiative heat flux density profile is shown in Fig. 5(b). The external sensible heat load of each room is depicted in Fig. 5(c).

The certainty internal sensible and latent heat loads and the CO_2 emission load of each room over a 24-hour period are predicted in Fig. 6. The certainty loads mean the sensible heat and moisture loads from lighting, equipment and applications. The values of Figs. 5-6 at every hour are commensurately quantized for the lower layer.

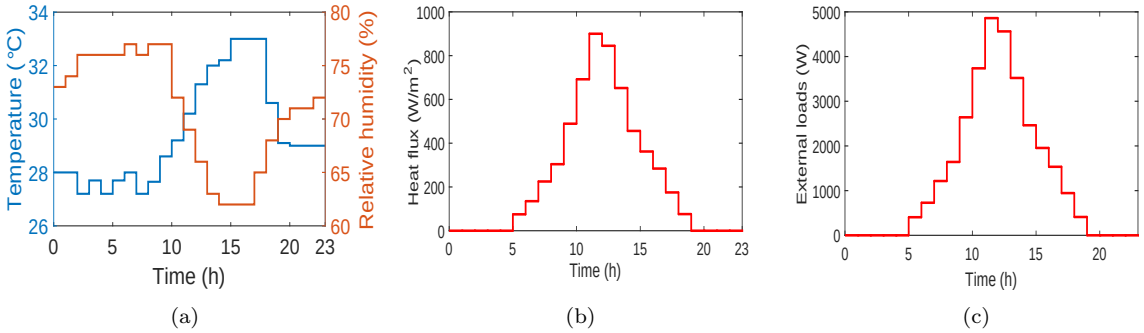

Figure 5: (a) Outside temperature and relative humidity. (b) Radiative heat flux. (c) External sensible heat load.

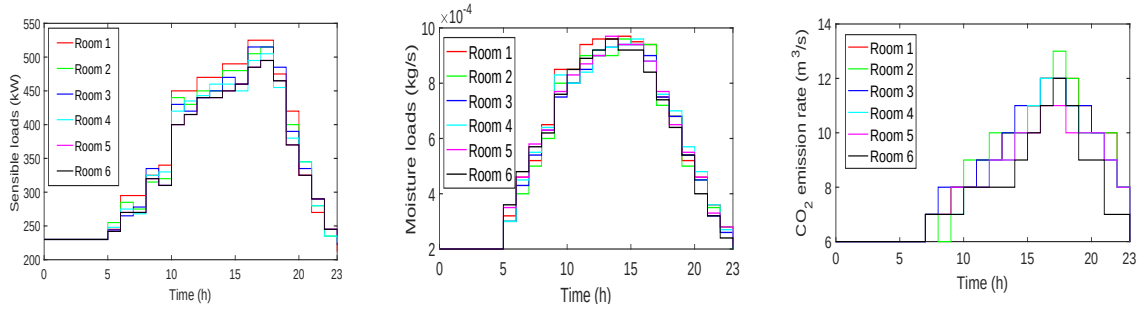

Figure 6: Certainty internal sensible, certainty moisture and CO_2 emission loads.

It is assumed that the building operates under the TOU rate plan shown in Table 5. Since there is a big difference in the demand charges between peak and off-peak hours, energy cost savings can be expected if significant amounts of peak power consumption are shifted to non-peak hours.

Table 5: Time-of-use electricity rates.

Summer	Period	Energy charge ($/kWh)	Demand charge ($/kWh)
Peak	12:00-18:00	0.20538	11.889
Standard	08:00-12:00, 18:00-21:00	0.05948	2.352
Off-Peak	21:00-08:00	0.03558	1.007

4.2. Comparison of optimal scheduling control strategies

To illustrate the performance of the proposed AHDC, comparisons with other control strategies are considered for scheduling the operation of the multi-zone building ME A/C system. The first approach is the DMPC algorithm based on given setpoints of air temperature, humidity and CO_2 concentration, aiming at minimizing energy consumption, referred as S1 [11]. The second approach is the DMPC algorithm based on energy cost and the value of the PMV index minimization, referred as S2 [12]. The proposed approach is the DMPC algorithm based on demand and energy cost minimization, referred as S3. To simplify the

comparison, among the three strategies, the multi-zone building ME A/C system operation profiles are generated by employing an NLP algorithm under the same outside and inside conditions. The control parameters are listed below: The sampling time $\Delta = 2$ minutes is adopted to discretize the nonlinear multi-zone building ME A/C system. The prediction horizon of the lower layer DMPC scheme is set as $N = 15$; the sampling periods of UOPC and LDMPC are 1 hour and 2 minutes, respectively. The total simulation time K^u is 24 hours. To illustrate the sampling period without affecting the control accuracy, the steady state solutions under the sampling periods 1 hour and 0.5 hour are plotted in Fig. 7. It can be seen from Fig. 7 that the control accuracy is rarely affected by the setting sampling period. Table 6 lists the combinations of the optimization and control strategies in the three scenarios. The test results for the three scenarios are shown in Section 4.3.

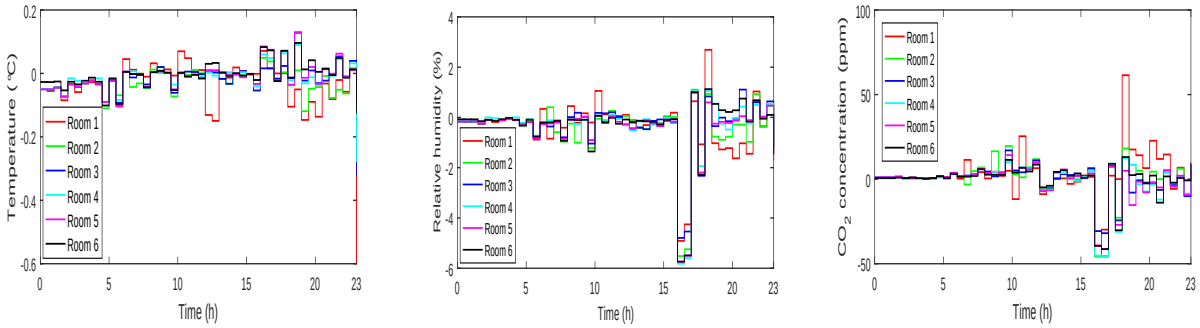

Figure 7: The steady state errors in six-room building under the sampling periods 1 hour and 0.5 hour.

Table 6: Comparison of different control strategies.

Scenarios	Upper layer optimization	Low layer control	Setpoint	DR action
S1	Energy consumption	DMPC	Given	
S2	Energy cost+PMV	DMPC	Autonomous	
S3	Energy cost+demand cost	DMPC	Autonomous	✓

4.3. Simulation test results

The performances of the three scenarios are compared through MATLAB simulations with historical weather data for a specific day. Fig. 8 shows the steady state profiles of air temperature, relative humidity and CO_2 concentration of each room, which are obtained by solving the distributed coordination optimization problem (22) and the centralized optimization (21). It can be seen from Fig. 8 that the distributed steady state is close to the centralized steady states of each room; the deviations are small and can be accepted by occupants (Assumption 1 is valid). The scheduling is thus effective.

The tracking reference points of the air temperature of each room with the three control strategies are depicted in Fig. 9 over a 24-hour period. The tracking reference points of relative humidity of each room with the three control strategies are illustrated in Fig. 10 over a 24-hour period. The tracking reference points of CO_2 concentration of each room with the three control strategies are shown in Fig. 11. Figs. 9-11 also show that the optimized reference points are adaptively preprogrammed by employing scenarios S2 and S3. We observe that each room's air temperature, relative humidity and CO_2 concentration, by using the proposed control strategy, are tracking and maintaining their reference points. It can be seen from Figs. 9-11 that the reference points of air temperature, relative humidity and CO_2 concentration of each room with scenarios S2 and S3 are raised during standard hours. The reason is that the controllers of scenarios S2 and S3 are automatically adjusting their reference points upward during standard hours according to the energy price policy and DR action respectively, such that the energy cost and energy consumption are minimized

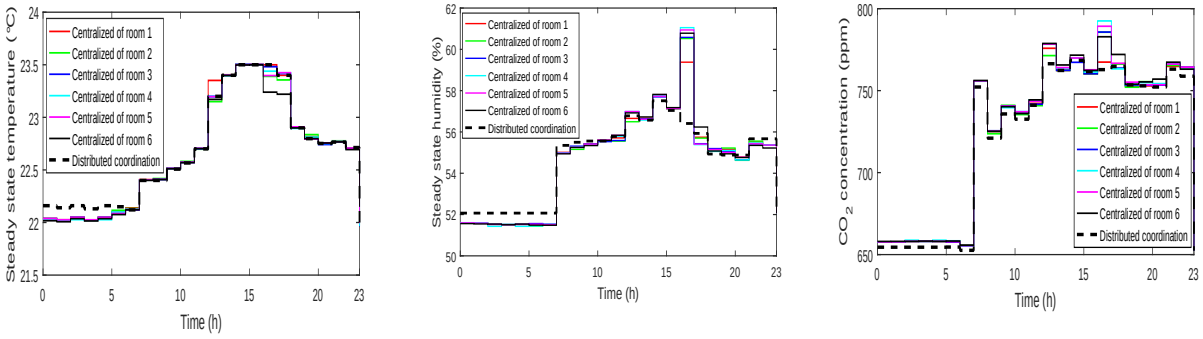

Figure 8: The steady state in each room under the distributed and centralized optimal controller.

while both thermal comfort and IAQ are still maintained within comfort ranges. The pre-cooling and pre-decreasing CO_2 contaminant concentration automatically starts in the morning simultaneously. This is because the energy costs for operating a multi-zone building ME A/C system during off-peak hours are lower than other periods. In the morning, the air temperature, humidity and CO_2 concentration reference points of all rooms are kept at the lower bounds of the comfort regions to store cooling and lower CO_2 contaminant concentration until the peak hours. As soon as the peak hours start, the reference points increase to the upper bounds, hence minimizing the demand in the afternoon by taking DR action. After more cooling and pollutant loads occur simultaneously during peak hours, the reference points are automatically set higher to turn off the cooling and increase the CO_2 contaminant concentration. We also observe that the time-varying reference points of air temperature, relative humidity and CO_2 concentration of each room are always maintained in the comfort regions over a 24-hour period with the proposed control strategy. We further observe that after reaching their reference points, the proposed controllers are maintaining the reference points with small variation ranges. Therefore, the proposed control strategy is capable of handling the changing cooling and pollutant loads over a 24-hour period and maintaining thermal comfort and IAQ at comfort levels. From Fig. 12, it can be observed that the values of the PMV index for the six rooms lie within the expected range [-0.5,0.5], which indicates that the indoor air temperature, humidity and CO_2 concentration are controlled within their comfort ranges. It can be observed from Fig. 12, with the control method in [40], the PMV index is controlled at the desired value, which indicates that the indoor air temperature and humidity are at their desired references, but it may not demonstrate that the indoor air CO2 concentration is within a comfort range.

Table 7: Comparison of different control strategies.

Strategy	Energy consumption (kWh)	Energy cost ($)
S1	124.56	10.67
S2	80.34	6.98
S3	79.78	5.66

To show the advantage of the proposed AHDC strategy over the other two control strategies in shifting demands from peak periods to non-peak periods, the power consumption under the peak and non-peak periods for the three control strategies are shown in Fig. 13. Table 7 summarizes the total energy consumption and cost for the multi-zone building ME A/C system under the three control strategies. From Table 7, it can be seen that with control strategies S2 and S3, more energy consumption and costs are reduced in comparison with control strategy S1. The reason is that each room's air temperature, humidity and CO_2 concentration reference points are adaptively and optimally preprogrammed under control strategies S2 and S3. We observe from Fig. 7 that the energy consumptions with control strategies S2 and S3 are almost the

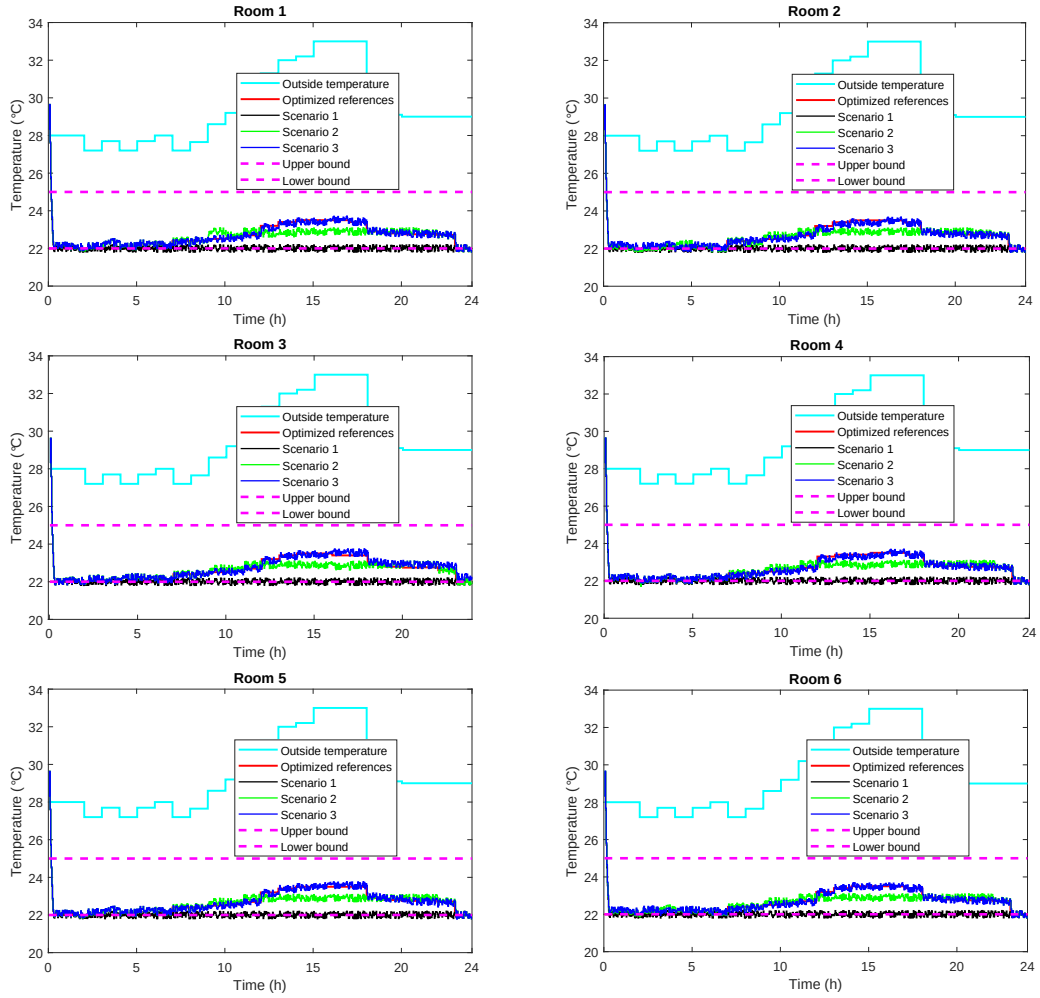

Figure 9: Each zone's temperature profile for a 24-hour period.

same, while the energy costs are different. It implies that the proposed control strategy S3 is capable of reducing more energy costs but not of reducing energy consumption in comparison with control strategy S2. It can be seen from Fig. 13 that under the proposed control strategy S3 with DR action, more energy costs are reduced during peak hours in comparison with control strategies S1 and S2. The reason is that the proposed control strategy S3 is automatically shifting peak demands to non-peak periods. Meanwhile, energy consumption with the proposed control strategy S3 is more than that with control strategy S2 during standard periods because the energy cost in standard periods is lower than that in peak periods. Consequently, minimizing total energy costs and shifting demand are achieved over a 24-hour period while maintaining both thermal comfort and IAQ at the required levels. Therefore, according to the above comparisons, the proposed control strategy S3 achieves a lower proportion of demand cost during peak hours and shows successful demand shifting and energy cost reduction.

Furthermore, to show the performance of the proposed distributed control strategies over the previous distributed control scheme [25], we will compare the two control methods in view of energy efficiency in this section. The distributed control strategy in [25] is based on the given reference of indoor air temperature and a linearization system of the HVAC system with a solar plant by fixing the fancoil air speed. The distributed controller is then steered for the HVAC system to follow the given reference with minimizing energy consumption. In order to compare the two control strategies, the control scheme [25] should be

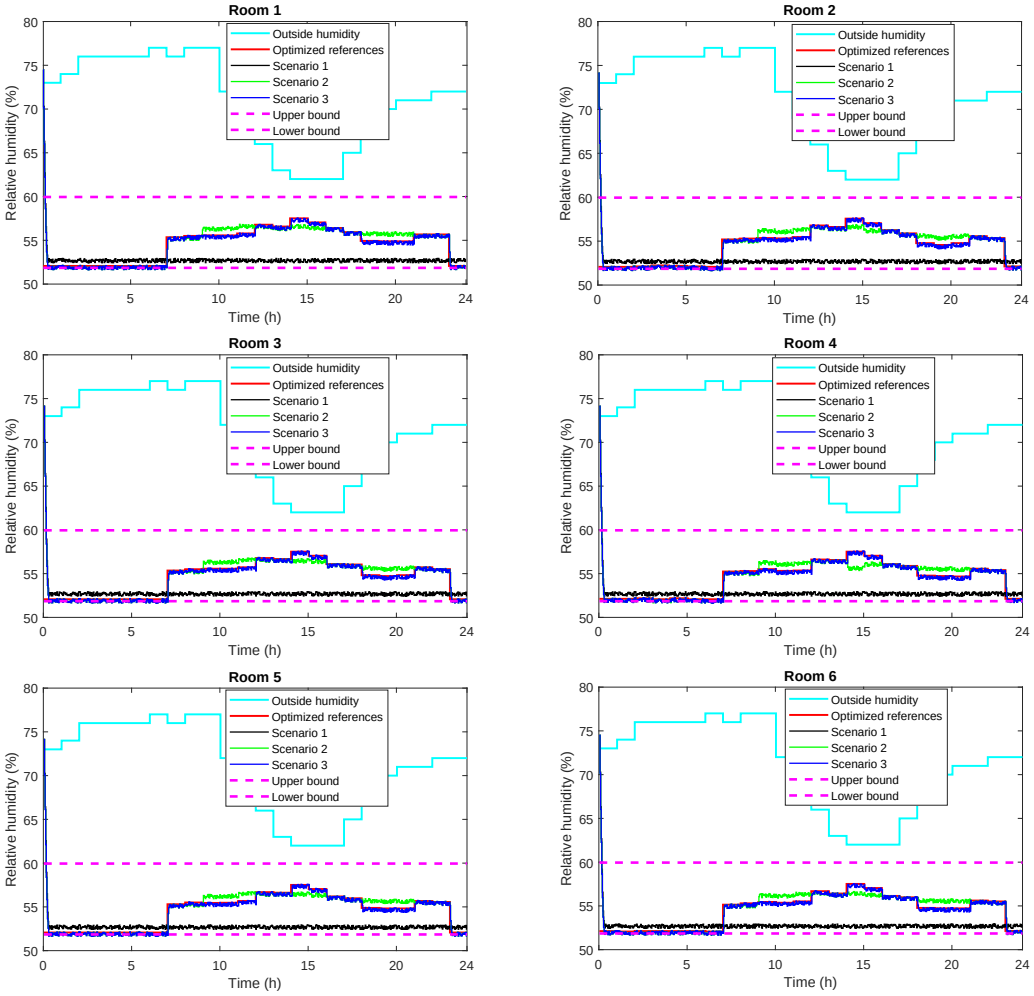

Figure 10: Each zone's relative humidity profile for a 24-hour period.

employed to steer the ME A/C system to follow the given reference and fixing volume flow rate of supply air. The comparison results are depicted in Table 8. It can be seen from the table that the proposed control strategy can reduce more energy consumption and cost in comparison with the previous control strategy [25]. The reason is that the proposed control scheme shifts the peak demand from the peak hours to off-peak hours by adaptively programming each room's setpoints of air temperature, humidity and CO_2 concentration.

Table 8: Compared with the previous control strategy.

Strategy	Energy consumption (kWh)	Energy cost ($)
Previous control [25]	128.75	10.98
Proposed control	79.78	5.66
Saving	38%	48.5%

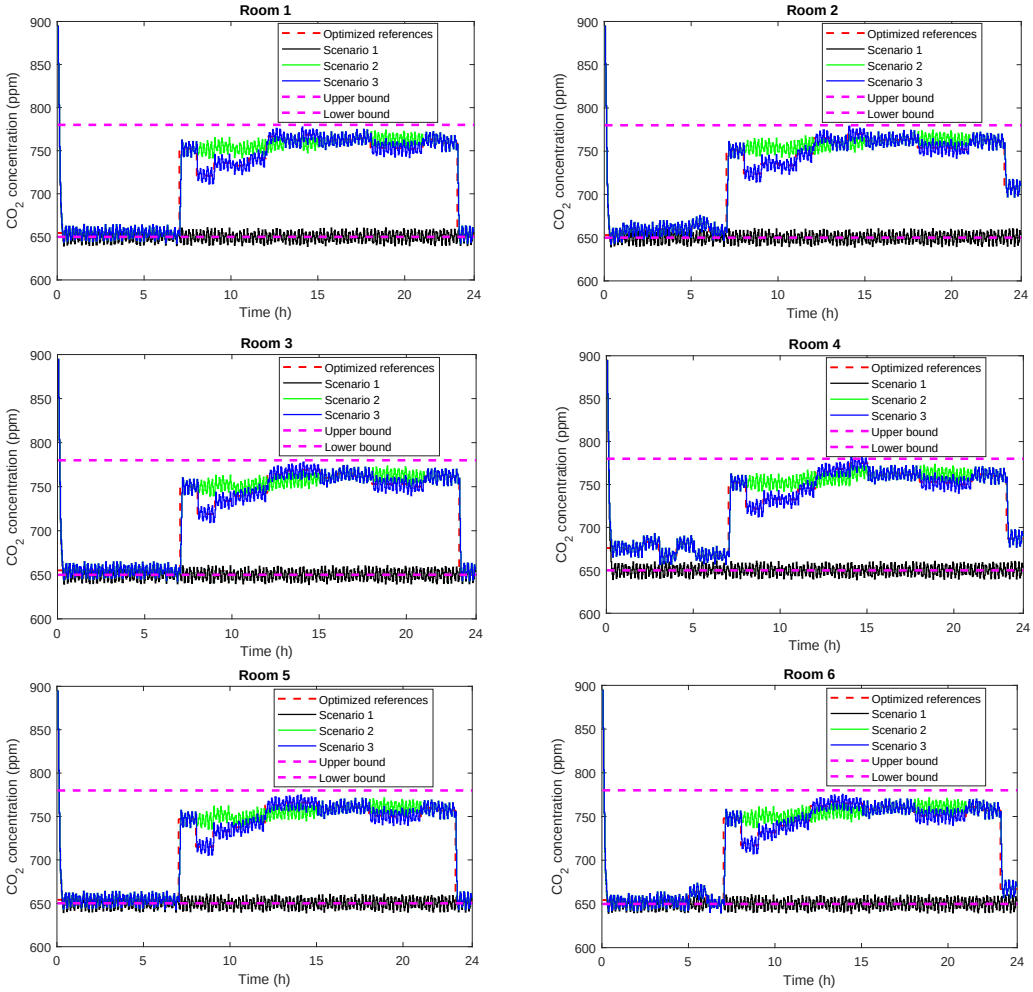

Figure 11: Each zone's CO_2 concentration profile for a 24-hour period.

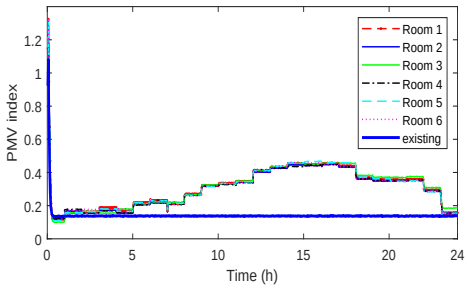

Figure 12: Profile of the value of the PMV index for the six rooms over a 24-hour period.

5. Conclusion

This paper presents an AHDC strategy to the problem of minimizing demand and energy costs, as well as reducing communication resources, computational complexity and conservativeness for a multi-zone building ME A/C system while maintaining both thermal comfort and IAQ within comfort ranges. The

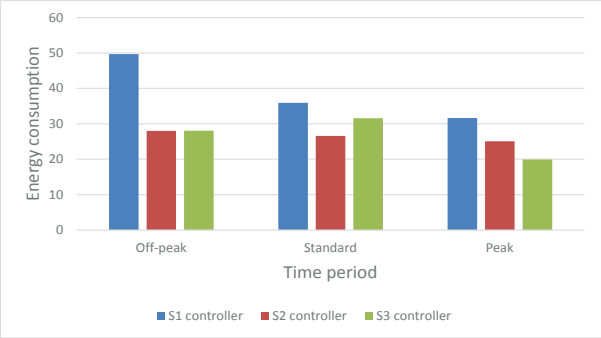

Figure 13: Energy consumption in three time periods with the three control strategies.

developed control strategy is an improvement over the current control methods, in which the air temperature, humidity and CO_2 concentration references of each zone are adaptively preprogrammed optimal operation profiles for the multi-zone ME A/C system to minimize the energy and demand costs. The lower layer DMPC controllers steer the multi-zone building ME A/C system to follow and maintain the autonomously preprogrammed references; meanwhile, the energy and demand costs are reduced and shifted from the peak hours to non-peak hours. The simulation results show that the designed DMPC controller optimise the transient processes reaching the steady state and over the previous distributed control method in view of energy efficiency. They also demonstrated that the proposed AHDC strategy gives the controller the ability to handle model parameters uncertainty and time-varying weather conditions. The proposed control strategy is suitable for a cluster of similarly purposed buildings, thus requiring less and cheaper communication resources to implement.

References

[1] UNEP Sustainable Buildings & Climate Initiative, Building and climate change: Summary for decision-makers, Paris CEDEX 09, France: Sustainable United Nations, 2009.

[2] K. Lee, J.E. Braun, Development of methods for determining demand-limiting setpoint trajectories in buildings using short-term measurements, Building and Environment, vol. 43, no. 10, pp. 1755-1768, 2008.

[3] R. Tang, S. Wang, K. Shan, H. Cheung, Optimal control strategy of central air-conditioning systems of buildings at morning start period for enhanced energy efficiency and peak demand limiting, Energy, vol. 151, pp. 771-781, 2018.

[4] S. Atthajariyakul, T Leephakpreeda, Real-time determination of optimal indoor-air condition for thermal comfort, air quality and efficient energy usage, Energy and Buildings, vol. 36, no. 7, pp. 720-733, 2004.

[5] M. Wallace, R. Mcbride, S. Aumi, P. Mhaskar, J. House, T. Salsbury, Energy efficient model predictive building temperature control, Chemical Engineering Science, vol. 69, no. 1, pp. 45-58, 2012.

[6] J. Cigler, S. Prívara, Z. Váňa, E. Žáčeková, L. Ferkl, Optimization of predicted mean vote index within model predictive control framework: Computationally tractable solution, Energy and Buildings, vol. 52, pp. 39-49, 2012.

[7] J. Mei, X. Xia, A reduced model for direct expansion air conditioning system and energy efficiency MPC control of indoor climate, in: 13th International Conference on Control and Automation, Ohrid, Macedonia, pp. 624-629, 2017.

[8] J. Ma, S.J. Qin, T. Salsbury, Application of economic MPC to the energy and demand minimization of a commercial building, Journal of Process Control, vol. 24, no. 8, pp. 1282-1291, 2014.

[9] M. Castilla, J. D. Álvarez, J. E. Normey-Rico, F. Rodríguez, Thermal comfort control using a non-linear MPC strategy: A real case of study in a bioclimatic building, Journal of Process Control, vol. 24, no. 6, pp. 703-713, 2014.

[10] M. Maasoumy, A. Sangiovanni-Vincentelli, Total and peak energy consumption minimization of building HVAC systems using model predictive control, IEEE Design and Test of Computers, vol. 29, no. 4, pp. 26-35, 2012.

[11] J. Mei, X. Xia, Energy-efficient predictive control of indoor thermal comfort and air quality in a direct expansion air conditioning system, Applied Energy, vol. 195, pp. 439-452, 2017.

[12] J. Mei, X. Xia, M. Song, An autonomous hierarchical control for improving indoor comfort and energy efficiency of a direct expansion air conditioning system, Applied Energy, vol. 221, pp. 450-463, 2018.

[13] F. Oldewurtel, A. Parisio, C.N. Jones, D. Gyalistras, M. Gwerder, V. Stauch, B. Lehmann, M. Morari, Use of model predictive control and weather forecasts for energy efficient building climate control, Energy and Buildings, vol. 45, pp. 15-27, 2012.

[14] M. Maasoumy, M. Razmara, M. Shahbakhti, A. Sangiovanni-Vincentelli, Handling model uncertainty in model predictive control for energy efficient buildings, Energy and Buildings, vol. 77, pp. 377-392, 2014.

[15] J. Hu, P. Karava, A state-space modeling approach and multi-level optimization algorithm for predictive control of multi-zone buildings with mixed-mode cooling, Building and Environment, vol. 80, pp. 259-273, 2014.
[16] M. Razmara, M. Maasoumy, M. Shahbakhti, R.D. Robinett III, Optimal exergy control of building HVAC system, Applied Energy, vol. 156, pp. 555-565, 2015.
[17] J. Mei, X. Xia, Multi-Zone building temperature control and energy efficiency using autonomous hierarchical control strategy, 2018 IEEE 14th International Conference on Control and Automation, Alaska, USA, pp. 884-889, 2018.
[18] M. S. Elliott, B. P. Rasmussen, Decentralized model predictive control of a multi-evaporator air conditioning system, Control Engineering Practice, vol. 21, no. 12, pp. 1665-1677, 2013.
[19] E. Atam, Decentralized thermal modeling of multi-zone buildings for control applications and investigation of submodeling error propagation, Energy and Buildings, vol. 126, pp. 384-395, 2016.
[20] X. Zhang, W. Shi, B. Yan, A. Malkawi, N. Li, Decentralized and distributed temperature control via HVAC systems in energy efficient buildings, arXiv preprint arXiv:1702.03308, 2017. [Online]. Available: https://arxiv.org/abs/1702.03308.
[21] Y. Zheng, S. Li, H. Qiu, Networked coordination-based distributed model predictive control for large-scale system, IEEE Transactions on Control Systems Technology, vol. 21, no. 3, pp. 991-998, 2013.
[22] P. Morosan, R. Bourdais, D. Dumur, J. Buisson, Building temperature regulation using a distributed model predictive control, Energy and Buildings, vol. 42, no. 9, pp. 1445-1452, 2010.
[23] Y. Ma, G. Anderson, F. Borrelli, A distributed predictive control approach to building temperature regulation, 2011 American Control Conference, pp. 2089-2094, 2011.
[24] P.D. Morosan, R. Bourdai, D. Dumur, J. Buisson, A distributed MPC strategy based on Benders' decomposition applied to multi-source multi-zone temperature regulation, Journal of Process Control, vol. 21, no. 5, pp. 729-737, 2011.
[25] H.F. Scherer, M. Pasamontes, J.L. Guzmán, J.D. Álvarez, E. Camponogara, J.E. Normey-Rico, Efficient building energy management using distributed model predictive control, Journal of Process Control, vol. 24, no. 6, pp. 740-749, 2014.
[26] Y. Long, S. Liu, L. Xie, K. H. Johansson, A hierarchical distributed MPC for HVAC systems, 2016 American Control Conference, pp. 2385-2390, 2016.
[27] N. Radhakrishnan, S. Srinivasan, R. Su, K. Poolla, Learning-based hierarchical distributed HVAC scheduling with operational constraints, IEEE Transactions on Control Systems Technology, vol. 26, no. 5, pp. 1892-1900, 2018.
[28] A. Zafra-Cabeza, J.M. Maestre, M.A. Ridao, E.F. Camacho, L. Sánchez, A hierarchical distributed model predictive control approach to irrigation canals: A risk mitigation perspective, Journal of Process Control, vol. 21, no. 5, pp. 787-799, 2011.
[29] X. Xu, P. Yan, S. Deng, L. Xia, M. Chan, Experimental study of a novel capacity control algorithm for a multi-evaporator air conditioning system, Applied Thermal Engineering, vol. 50, no. 1, pp. 975-984, 2013.
[30] V. Vakiloroaya, Q.P. Ha, M. Skibniewski, Modeling and experimental validation of a solar-assisted direct expansion air conditioning system, Energy and Buildings, vol. 66, pp. 524-536, 2013.
[31] M.J. Jiménez, H. Madsen, K.K. Andersen, Identification of the main thermal characteristics of building components using MATLAB, Building and Environment, vol. 43, no. 2, pp. 170-180, 2008.
[32] P. Bacher, H. Madsen, Identifying suitable models for the heat dynamics of buildings, Energy and Buildings, vol. 43, no. 7, pp. 1511-1522, 2011.
[33] Y. Ma, J. Matuško, F. Borrelli, Stochastic model predictive control for building HVAC systems: Complexity and conservation, IEEE Transactions on Control Systems Technology, vol. 23, no. 1, pp. 101-116, 2015.
[34] W. Chen, S. Deng, Development of a dynamic model for a DX VAV air conditioning system, Energy Conversion and Management, vol. 47, no. 48-49, pp. 2900-2924, 2006.
[35] Q. Qi, S. Deng, Multivariable control-oriented modeling of a direct expansion (DX) air conditioning (A/C) system, International Journal of Refrigeration, vol. 31, no. 5, pp. 841-849, 2008.
[36] H. Yu, X. Xia, Adaptive leaderless consensus of agents in jointly connected networks, Neurocomputing, vol. 241, pp. 64-70, 2017.
[37] V. Vakiloroaya, B. Samali, K. Pishghadam, Investigation of energy-efficient strategy for direct expansion air-cooled air conditioning systems, Applied Thermal Engineering, vol. 66, no. 1-2, pp. 84-93, 2014.
[38] P.O. Fanger, Thermal Comfort: Analysis and Applications in Environmental Engineering, Copenhagen, Denmark: Danish Technical Press, 1972.
[39] M. Castilla, J.D. Álvarez, M. Berenguel, F. Rodríguez, J.L. Guzmán and M. Pérez, A comparison of thermal comfort predictive control strategies, Energy and Buildings, vol. 43, no. 10, pp. 2737-2746, 2011.
[40] R.Z. Freire, G.H.C. Oliveira, N. Mendes, Predictive controllers for thermal comfort optimization and energy savings, Energy and Buildings, vol. 40, no. 7, pp. 1353-1365, 2008.
[41] S. Wang, X. Jin, Model-based optimal control of VAV air-conditioning system using genetic algorithm, Building and Environment, vol. 35, no. 6, pp. 471-487, 2000.
[42] K. Gladyszewska-Fiedoruk, Correlations of air humidity and carbon dioxide concentration in the kindergarten, Energy and Buildings, vol. 62, pp. 45-50, 2013.
[43] S. Lin, S. Chiu, W. Chen, Simple automatic supervisory control system for office building based on energy-saving decoupling indoor comfort control, Energy and Buildings, vol. 86, pp. 7-15, 2015.
[44] J.B. Weir, New methods for calculating metabolic rate with special reference to protein metabolism, The Journal of Physiology, vol. 109, pp. 1-9, 1949.
[45] J.M. Kinney, A.P. Morgan, F.J. Domingues, K.J. Gildner, A method for continuous measurement of gas exchange and expired radioactivity in acutely III patients, Metabolism, vol. 13, no. 3, pp. 205-211, 1964.
[46] C.C. Christensen, H.M.M. Frey, E. Foenstelien, E. Aadland, H.E. Refsum, A critical evaluation of energy expenditure estimates based on individual O2 consumption/heart rate curves and average daily heart rate, The American Journal of Clinical Nutrition, vol. 37, no. 3, pp. 468-472, 1983.

[47] M.S. Treuth, A.L. Adolph, N.F. Butte, Energy expenditure in children predicted from heart rate and activity calibrated against respiration calorimetry, American Journal of Physiology-Endocrinology and Metabolism, vol. 275, no. 1, pp. 12-18, 1998.

[48] N. Djongyang, R. Tchinda, D. Njomo, Thermal comfort: A review paper, Renewable and Sustainable Energy Reviews, vol. 14, no. 9, pp. 2626-2640, 2010.

[49] X. Xia, J. Zhang, and A. Elaiw, An application of model predictive control to the dynamic economic dispatch of power generation, Control Engineering Practice, vol. 19, pp. 638-648, 2011.

[50] J. Zhang, X. Xia, A model predictive control approach to the periodic implementation of the solutions of the optimal dynamic resource allocation problem, Automatica, vol. 47, no. 2, pp. 358-362, 2011.